Escuela Técnica Superior de ingenieros
industriales y de telecomunicación

UNIVERSIDAD DE CANTABRIA

Trabajo Fin de Máster

Sobre la desinfección de superficies por radiación UVC: un análisis numérico y experimental

(On the surface disinfection with UVC radiation: a numerical and experimental analysis)

Para acceder al Título de

Máster Universitario en Ciencia e Ingeniería de la Luz

Autor: Beatriz Menéndez López
Directores: Fernando Moreno Gracia
y Alfredo Franco Pérez

Septiembre 2021

If at first I did not write a dedication to this document, it is because I do not have the words to express my gratitude to all who have accompanied me on this path, for their patience and dedication.

Resumen

El constante desarrollo tecnológico y la creciente necesidad de protección ante la propagación de enfermedades cada vez más rápida debido a la globalización, ha propiciado el uso de radiación ultravioleta C (UVC) como herramienta de desinfección. Este documento pretende servir como guía para el uso de radiación UVC en la desinfección de superficies, introduciendo los conceptos básicos que permiten entender cómo esta radiación puede inactivar microorganismos y su grado de efectividad. Para ello, se realiza un estudio radiométrico mediante simulación de trazado de rayos que se compara con cálculos numéricos y medidas experimentales. Además, se trata la interacción de la radiación con material biológico y se analiza el daño causado sobre una muestra de ADN, una secuencia del gen ODZ1.

Palabras clave: ultravioleta, desinfección, UVC, radiometría, dosimetría

Abstract

The constant technological development and the growing need for protection against the increasingly rapid spread of diseases due to globalisation have led to the use of ultraviolet C (UVC) radiation as a disinfection tool. This document aims to serve as a guide for the use of UVC radiation in the disinfection on surfaces, introducing the basic concepts that allow us to understand how this radiation can deactivate microorganisms and its degree of effectiveness. To this end, a radiometric study is carried out using ray-tracing simulation, which is compared with numerical calculations and experimental measurements. Moreover, the radiation-biological matter interaction is discussed, and the damage caused to a DNA sample, a sequence of the ODZ1 gene, is analysed.

Keywords: ultraviolet, disinfection, UVC, radiometry, dosimetry

Contents

1 Introduction **1**
1.1 Main objectives . . . 4

2 Theoretical background **6**
2.1 Electromagnetic radiation . . . 6
2.1.1 Radiometry . . . 8
2.1.2 Electromagnetic spectrum and ultraviolet radiation . . . 11
2.2 Radiation-matter interaction . . . 12
2.2.1 Biological medium . . . 15
2.3 Disinfection methods . . . 16
2.4 Methods of calculus . . . 17
2.4.1 Ray tracing simulations . . . 18

3 Radiometric analysis **21**
3.1 Parallelepipedic geometry . . . 21
3.2 Characterization and use of a luminaire . . . 25
3.2.1 Lamp response . . . 27
3.2.2 Dosimetry . . . 30

4 Biodosimetric analysis **35**
4.1 Microorganism response . . . 35
4.1.1 UVC disinfection effectiveness . . . 35
4.1.2 Mathematical models . . . 37
4.2 Protocol of samples . . . 38
4.2.1 DNA sample preparation . . . 39
4.2.2 Irradiation, analysis and germicidal effect on ODZ1 . . . 40

5 Conclusions and future work **48**

A Luminaire geometry **54**

B Irradiation protocol **56**

C Matlab codes **58**

D Gene sequencing **62**

Chapter 1

Introduction

Disinfection is a sort of treatment to reduce the number of microorganisms, helping to prevent illness and the spread of germs, which has become more and more important due to globalization. The most relevant example that has awakened many consciences is the COVID-19 pandemic, which entails the creation of new prevention protocols, not only for the healthcare field but also for the broad audience. A disinfection tool growing in importance for the last few years is ultraviolet C radiation, because of its effectiveness, non-toxicity, easiness of use, and speed.

In 1665 Newton started to make experiments with a prism, spreading a white light beam into visible colours by dispersion. This experiment changed the way to understand light and allowed us to investigate beyond the limits of visible light leading to the concept of electromagnetic spectrum coined by James Clerk Maxwell but discovered by William Herschell while investigating the relation between light and heat [1].

Inspired by Herschell's discovery, Wilhelm Ritter discovered ultraviolet light in 1801 while investigating the energy of light from different parts of the spectrum beyond violet visible limits. The properties and limits of the ultraviolet range were refined during the 19^{th} and the early 20^{th} centuries, with important contributions as the map of sunlights bands of Fraunhofer or the invention of the spectroscope by Kirchoff and Bunsen to know the light absorption of different atoms as a function of the wavelength [2].

Although the main source of light par excellence, the sun, emits in the ultraviolet range, this part was unnoticed throughout history due to absorption bands in the atmosphere, where the ozone absorbs ultraviolet C radiation and partially ultraviolet B radiation. Ultraviolet radiation is located in the electromagnetic spectrum between X-Rays and visible light, hence it is invisible to the human eye. The exposure of eyes and skin to far ultraviolet radiation (UVC) is very dangerous because of its ability to damage the genetic material of every cell.

The discovery of ultraviolet radiation and its blockage by the upper atmosphere boosted the development of UV lamps to continue the field of study. The characteristics and possible uses of ultraviolet light emerged after Wheatstone invention of the mercury vapor lamp in 1835 [2], which was brighter than previous arc lamps. These range from calibration sources because of the narrow peaks of its emission spectrum, to disinfection because of its germicidal effect, which is the main point of this work.

The first observation of germicidal effects of ultraviolet radiation began with Downes and Blunt in 1877, who reported bacteria inactivation by sunlight, and according to von Recklinghausen the first use to disinfect drinking water was done in 1906 [3]. Those investigations spread out to the present days appearing in the form of disinfection applications of water, air, and surfaces.

This germicidal ability of ultraviolet C light means that it can be used as a disinfection tool because it is usually able to deactivate more than 99% of bacteria and other pathogenic microorganisms. However, the disinfection concept must not be confused with the sterilization concept, which implies the 100% kill or deactivation of all forms of life [4]. The germicidal effectiveness of ultraviolet radiation is a function of many different parameters such as distance to the source of light, dose, exposure time, orientation, material, shadows, among others [5].

Ultraviolet C radiation has this germicidal capability because it is strongly absorbed by most of the organic matter. This absorbed energy is large enough to break chemical bonds and to ionize atoms and molecules, which cause damage in molecules, cellular processes deactivation and the death of microorganisms.

To understand how ultraviolet light can cause damage in live matter such as microorganisms, we first have to know the composition and function of organisms.

The key of every organism is its genetic material, which is kept in two types of nucleic acids, DNA or RNA. Nucleic acids of cells and viruses carry the instructions for cells functions as growth, reproduction and death.

The germicidal ultraviolet wavelength range overlaps with the absorbance peak of DNA and RNA, which is around 260 nm (see *Fig. 1.1*). Thus, the absorbed energy will produce changes in the genetic material and therefore creates transcription errors and deactivates processes if the damage is high enough [6].

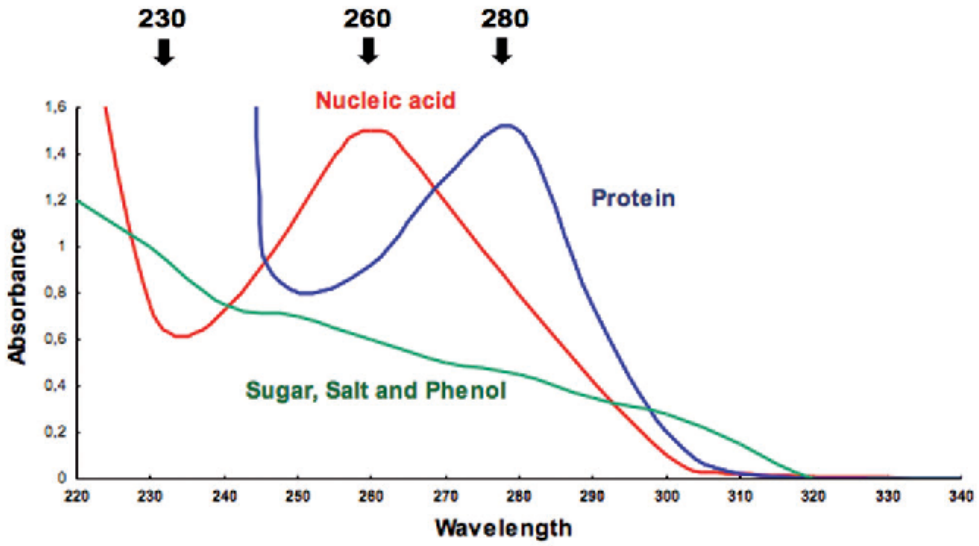

Figure 1.1: Absorption spectrum of nucleic acid and proteins [7].

Nucleic acids are polymers formed by the repetition of nucleotides linked by phosphodiester bonds (a type of covalent bond that occurs between a hydroxyl group $OH-$ and a phosphate group). The basic molecules of the genetic material are called nucleotides, which contain a phosphate group, a sugar group and one of the nitrogenous bases, also called nucleobases. There are five nucleobases: adenine (A), guanine (G), cytosine (C), thymine (T) and uracil (U), whose structure is shown in *Fig. 1.3*. Adenine and guanine have a similar structure and they are named purine bases. Cytosine, thymine and uracil are also similar between them and they are called pyrimidine bases [8].

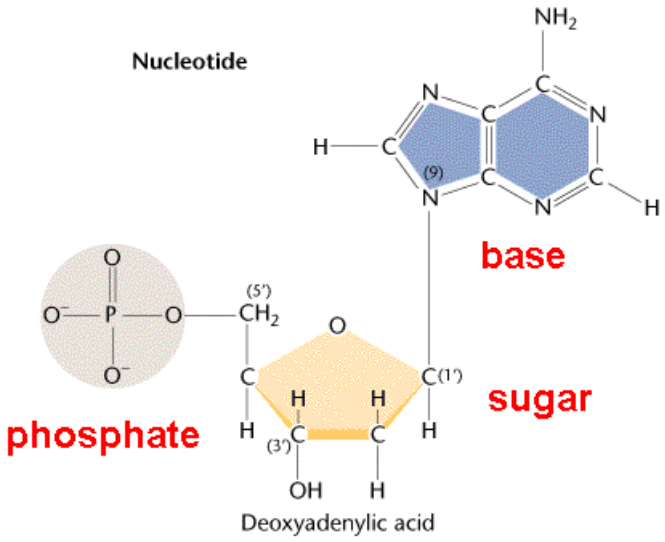

Figure 1.2: Structure of a nucleotide [9].

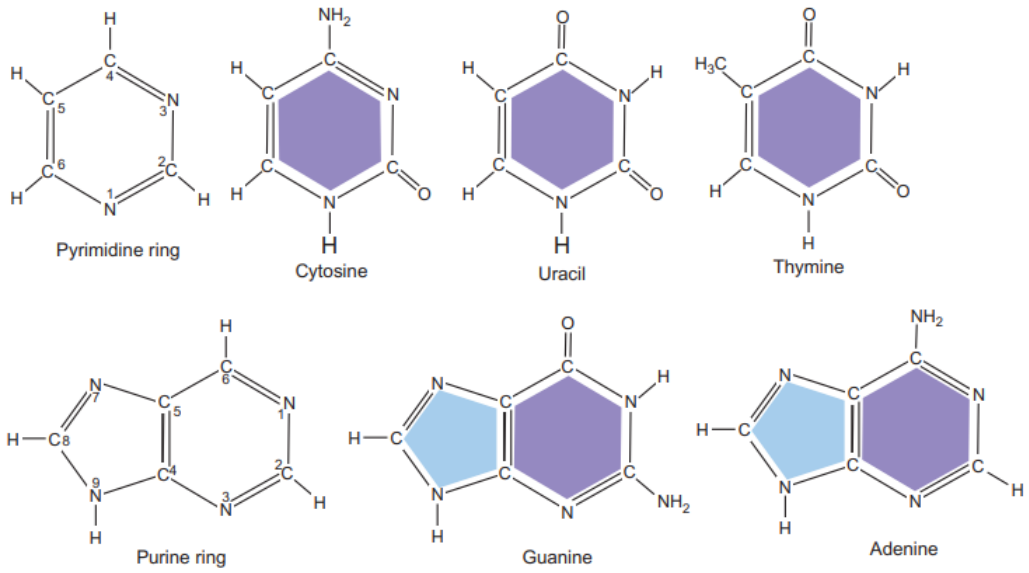

Figure 1.3: Nucleobase structure [10].

The difference between DNA and RNA is the sugar associated, deoxyribose or ribose respectively. Usually, RNA consists of a single nucleic acid chain, but DNA has two chains linked by hydrogen bonds between base pairs, G with C (triple bonds) and A with T (double bonds), and the thymine is replaced by the uracil in the RNA [11].

The sequence of the different bases is translated into specific proteins necessary for cellular functions. Small modifications in these sequences (mutations) can cause errors in the formation of these proteins, causing significant changes in cellular processes. Therefore, to deactivate a microorganism, to stop its reproduction or even to kill it, it will be crucial to cause damage in its genetic code and the compounds associated with the reparation mechanisms.

1.1 Main objectives

The main objective of this work is to understand the basics of ultraviolet disinfection and to create an effective methodology to verify the germicidal capacity of disinfection devices. This work is focused on the study of ultraviolet C radiation as a disinfection tool and also on how to validate its germicidal effect. The procedure followed in this study consists of 5 steps:

First, a ray tracing software must be checked, by taking a lamp with known properties, simulating its radiation pattern, and comparing it with the radiation numerical calculus for this lamp.

Second, once the consistency of the simulation has been proved by physical models, the radiation is measured from real lamps to fine adjust the ideal parameters given by the manufacturer to real radiation values.

Third, the lamp radiation is simulated on several surfaces distributed inside different closed rooms. The accumulated energy density dose received by each surface is calculated, taking into account the exposure time, the position of the light source, and the stabilization curve of the lamp.

Fourth, the radiation pattern is checked in real environments through different measurements tools: electronic radiometer, chemical dosimeters and biodosimeters.

Fifth, the chemical dosimeters measurements are interpreted by means of a colourimetric analysis based on a colour-dose calibration, and the biodosimeters response is analyzed considering specific pathogens dependant damage-dose relations.

This specific list of steps is proposed as the operational method to deal with the key goals:

- To characterise ultraviolet radiation sources, in particular low pressure mercury vapor lamps.
- To simulate the radiation pattern at 254 nm in wavelength of lamps and luminaries by means of ray tracing.
- To calibrate chemical dosimeters based on electronic radiometer measurements and also based on computational simulations.
- To study the effect of different UVC radiation doses on genetic material.

The computing system used all over this work is Photopia, from LTI Optics, which is a software based on ray tracing analysis. Every single step of the process serves to enhance the usefulness of simulations, and to speed up the calculus to validate the germicidal capacity of any ultraviolet radiation source in any kind of closed space.

The work done for reaching the steps of the operational method is collected into different chapters according to its topic. *Chapter 2* contains the basis of ultraviolet radiation and its interaction with matter, especially with biological medium. Moreover, disinfection methods, radiometry concepts and methods of calculus needed for understanding how and why ultraviolet C radiation can be used as a disinfection method, are justified.

In *Chapter 3*, the simulation procedure is shown. Also, we explain the necessary concepts in order to properly analyse the results. Furthermore, luminaire characterization, the response of its lamps and how to use it to calibrate chemical dosimeters is described in detail. *Chapter 4* digs into the biological study with the general microorganisms response and the specific results of DNA damage in a gene of ODZ1. *Chapter 5* closes the work gathering up the conclusions of the analysis, giving rise to a process for using UVC devices as a disinfection tool and the way to validate its germicidal effect. The appendix contains geometrical considerations of the characterised luminaire, the irradiation, MatLab codes of chemical dosimeters calibration and the sequence of the gene.

Chapter 2

Theoretical background

Along this chapter, the theoretical basis of the electromagnetic radiation and the ultraviolet disinfection process are explained, following the guidelines of reference [3], from ultraviolet radiation definitions and its interaction with matter to the basic radiometric parameters, numerical calculus and simulations.

2.1 Electromagnetic radiation

Electromagnetic radiation consists of electromagnetic waves, which are composed of oscillating electric and magnetic perpendicular fields propagating through the space.

Throughout this thesis, we will use the term radiation to refer to electromagnetic radiation. In particular, we will focus on the ultraviolet range due to its disinfection properties.

Every kind of wave is described by the general equation of wavy movement, the wave equation, which for electromagnetic waves is a consequence of Maxwell's equations [12]. These equations represent the background of electricity and magnetism through mathematical expressions with space and time dependence that are usually presented in their differential form and were reduced by Heaviside to 4 equations: Gauss' Law for electricity, Gauss' Law for magnetism, Faraday-Lenz's Law and Ampère-Maxwell's Law, which expressions are respectively given by

$$\nabla \cdot \vec{E} = \frac{\rho}{\varepsilon_0} \tag{2.1}$$

$$\nabla \cdot \vec{B} = 0 \tag{2.2}$$

$$\nabla \times \vec{E} = -\frac{\partial \vec{B}}{\partial t} \tag{2.3}$$

$$\nabla \times \vec{B} = \mu_0 \vec{J} + \mu_0 \varepsilon_0 \frac{\partial \vec{E}}{\partial t} \tag{2.4}$$

where E represents the electric field, ρ is the charge density, ε_0 is the permittivity, B is the magnetic field, t is the time, μ_0 is the permeability and J is the current density. In vacuum, an electromagnetic wave propagates at the velocity c (speed of light) given by *Eq.* (2.5).

$$c = \frac{1}{\sqrt{\varepsilon_0 \cdot \mu_0}} \tag{2.5}$$

Solutions to Maxwell's equations depend on the optical properties of the materials, their electric permittivity, ε, and their magnetic permeability, μ. In our case, we are going to consider isotropic materials with no magnetic field impact, so we are going to consider only the electric field. The wave equation for the electric field is *Eq.* (2.6).

$$\frac{\partial^2 \vec{E}}{\partial x^2} + \frac{\partial^2 \vec{E}}{\partial y^2} + \frac{\partial^2 \vec{E}}{\partial z^2} = \frac{1}{c^2}\frac{\partial^2 \vec{E}}{\partial t^2} \tag{2.6}$$

The basic solutions of this equation (and the most important) are the plane waves and the spherical waves. In general, the linear character of this equation allows to write whatever other solution as a linear combination of the basic ones. Their expressions for plane and spherical waves are respectively given by *Eq.* (2.7) and *Eq.* (2.8).

$$\vec{E}(\vec{r}, t) = \vec{E_0} \cdot e^{i(w \cdot t \mp \vec{k} \cdot \vec{r})} \tag{2.7}$$

$$\vec{E}(\vec{r}, t) = \frac{\vec{E_0}}{r} \cdot e^{i(w \cdot t \mp k \cdot r)} \tag{2.8}$$

In *Eq.* (2.7), w is the angular frequency, t is the time, $\vec{k}$ is the vector wave ($|\vec{k}| = 2\pi/\lambda$ where λ is the wavelength), $\vec{r}$ is the vector of distance in the wave propagation direction. The sign convention used here describes a wave travelling towards positive r with the negative sign $(-k)$, and travelling towards negative r with the positive one $(+k)$ [13]. In *Eq.* (2.8), r is the distance to the source, the negative sign $(-k)$ represents emerging waves, and the positive one $(+k)$, collapsing waves.

Electromagnetic waves transport energy associated to the electric and magnetic fields as they travel through space. This transport of energy per unit time across the unit area is described by the Poynting vector $\vec{S}$ [14].

$$\vec{S} = \frac{1}{\mu_0}\vec{E} \times \vec{B} \tag{2.9}$$

The poynting vector is a magnitude that describes how much energy per second flows perpendicularly through a surface of one square meter, and also the direction of propagation of that energy. Although in this work we are interested in the analysis of the electromagnetic energy problem, which is what radiometry studies, it is important to mention that the direction of the Poynting vector, which indicates the trajectory of the wave in isotropic media, is also associated with the concept of **ray** (see *Section 2.4.1*). The energy per unit area will correspond with the ray's density.

In radiometry, the time average of the Poynting vector is the irradiance (E_e), also known as intensity (I), which is given by

$$I = \left| \langle \vec{S} \rangle \right| \tag{2.10}$$

So, the irradiance is proportional to the square of the amplitude of the electric field [15].

$$I \propto E_0^2 \tag{2.11}$$

If we substitute the solutions of the wave equation, *Eq.* (2.7) and *Eq.* (2.8), in *Eq.* (2.11), we obtain respectively a constant irradiance for the plane waves, $I \propto E_0^2$, and the attenuation of the amplitude with the square of distance for the spherical wave solution, $I \propto \frac{E_0^2}{r^2}$, i.e. the well-known inverse distance square law (see *Section 2.1.1*).

2.1.1 Radiometry

Electromagnetic radiation transports energy travelling as classical waves or photons. The corresponding energy distribution is studied by Radiometry. It involves the entire optical radiation spectrum.

As it happens for many different physical phenomena (e.g. gravity, heat or sound), for a point source, the radiation intensity is governed by the inverse square law. This is a strictly geometrical consideration, in which the intensity of a point radiation source decays as the square of the distance to the source due to the conservation of energy (see *Fig. 2.1*).

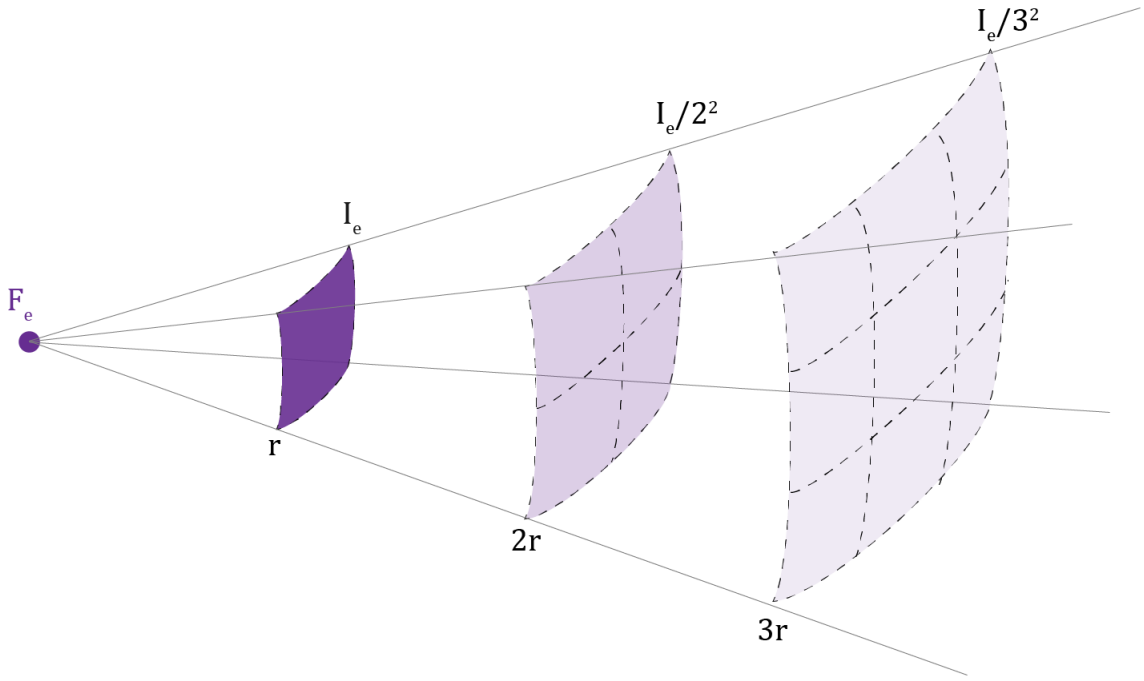

Figure 2.1: Representation of radiation attenuation due to inverse square law.

Although this law describes radiation attenuation, there are many complement terms and parameters concerning the source radiation study. Hence, below they are described to understand the use of radiation as a disinfection tool [15][16].

First of all, the term "lamp" will be used to refer to the light source, for instance, fluorescent tubes, LEDs, incandescent or halogen lamps. The proper technical term to define the

full device which is composed of at least one lamp, is "luminaire".

By considering radiometric parameters, the fundamental characteristic of a lamp is the **radiant flux** (or radiant power), F_e or ϕ, which is the total energy emitted in all directions per unit of time, so, it is measured in W. If the radiation emitter is a point source, the energy flux per unit of solid angle, $d\Omega$, is defined by the **radiant intensity**, I_e, and it is measured in W/sr (Watts per stereoradian).

On the other hand, radiated surfaces have also their own definitions for the energy received. The most important radiometric magnitude all over this work is the **irradiance**, E_e (also named I), which is the total received flow of energy in all directions onto an infinitesimal area, and therefore, its unit is W/m^2. Moreover, the **radiant exposure**, H_e, also denominated as **dose**, D, is crucial in the disinfection by UV radiation, since it is the parameter defining the total radiant energy passing through a small area of irradiated surfaces, and it is measured in J/m^2.

Once these parameters are known, we can make a simple model which allows us to calculate the irradiance at any point of the space by knowing the position and characteristics of the source. Assuming the lamp as a point source (*Fig. 2.2*), the radiant intensity is defined as *Eq.* (2.12),

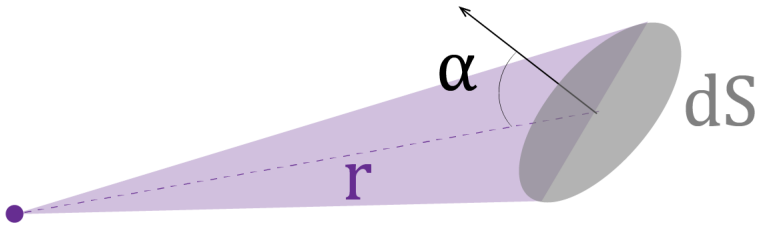

Figure 2.2: Point source radiating a surface dS.

$$I_e = \frac{dF_e}{d\Omega} = \frac{F_e}{4\pi} \tag{2.12}$$

$$d\Omega = \frac{dS \cdot \cos\alpha}{r^2} \tag{2.13}$$

$$E_e = \frac{dF_e}{dS} = \frac{I_e \cdot d\Omega}{dS} = \frac{F_e \cdot \cos\alpha}{4\pi \cdot r^2} \tag{2.14}$$

where r is the vector between the lamp position (X, Y, Z) and the object position (x, y, z), and α is the angle that r forms with the normal of the object plane. It can be written as a function of those coordinates as

$$r = \sqrt{(X-x)^2 + (Y-y)^2 + (Z-z)^2} \tag{2.15}$$

$$\cos\alpha = \frac{\|Z-z\|}{r} \tag{2.16}$$

Considering that most of the lamps used throughout this thesis are tube lamps, a more realistic model can be implemented by assuming the tube lamp as a line made of infinite point sources (see *Fig. 2.3*).

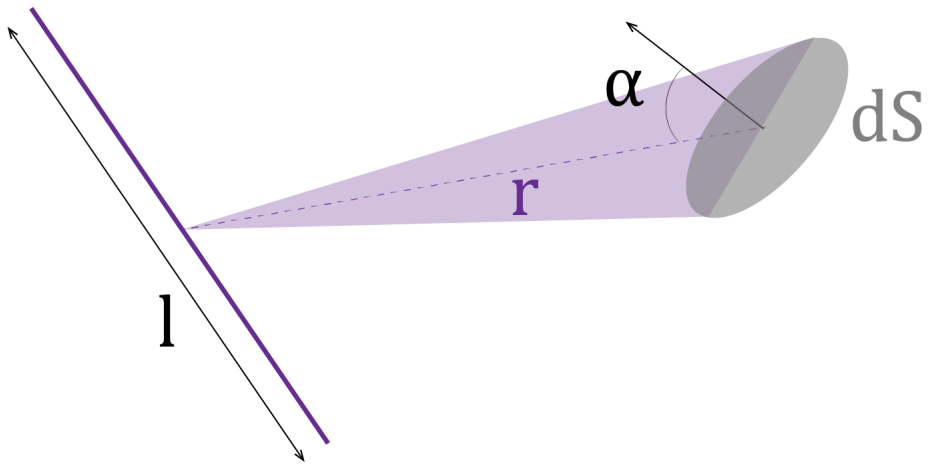

Figure 2.3: Line source radiating a surface.

$$I_e = \frac{F_e}{4\pi \cdot l} \tag{2.17}$$

$$E_e = \int \frac{F_e \cdot \cos\alpha}{4\pi \cdot r^2} dl \tag{2.18}$$

$$E_e = \int_{\frac{X-l}{2}}^{\frac{X+l}{2}} \frac{F_e \cdot \|Z - z\|}{4\pi \cdot r^3} dX \tag{2.19}$$

In addition to the calculated irradiance, as each material behaves differently in response to radiation, magnitudes as absorbance, reflectance or transmittance are taken into account in the radiometric study to analyse properly more realistic situations.

The best way to internalise the pattern of radiation and dose distribution is to keep in mind the radiation protection principles: distance, time, and shielding.

The dose is related to **distance** by the inverse square law, implying smaller radiant intensities for larger distances. Whereas irradiance is the dose per unit time, the dose is directly proportional to the exposure **time**. And finally, the radiation-matter interaction determines the absorbance of radiation and if a material can be used as **shielding** or not.

All in all, the distance to the source is the key factor to get the largest dose on a surface and to disinfect it in the shortest time. However, as it has been seen in *Eq.* (2.14) and *Eq.* (2.18), the irradiance that an object receives depends on the orientation with respect to the light source, this becoming a factor more relevant than the distance for surface disinfection, because the exposed area is angle dependant.

2.1.2 Electromagnetic spectrum and ultraviolet radiation

As previously stated, electromagnetic radiation propagates in form of waves and transports energy. As a wave, it is characterized by its frequency (or wavelength) and this allows to classify it according to this parameter. This classification constitutes the electromagnetic spectrum. This spectrum is divided into ranges, which in ascending order of energy are: radio waves, microwaves, infrared (IR), visible light, ultraviolet (UV), X-rays and gamma rays.

For ultraviolet radiation, there are several different classifications and none is adopted as universal, so the limits of each range are diffuse. Here we are going to adopt what we think is the most used. Ultraviolet radiation spans from 100 to 380 nm, and it can be separated into four bands, UVA (near UV) which covers from 320 to 380 nm, UVB (medium UV) from 280 to 315 nm, UVC (far UV) from 200 to 280 nm and VUV (vacuum UV) from 100 to 200 nm.

Except for the ultraviolet A band, ultraviolet radiation is considered actinic radiation, which means that when it interacts with matter it causes photochemical reactions. UVC and UVB bands are known as ultraviolet germicidal irradiation bands (UVGI) since they have a disinfection effect reducing the microbial population. These bands can cause damage, kill or inactivate microorganisms such as bacteria, viruses and fungi.

UVA radiation can easily transmit through air and glass, UVA band sources are also known as blacklights or Wood lamps, and they are used to detect cracks in surfaces, to activate molecules in the curing process, in industrial illumination, tanning beds or as insect traps [17] [18].

UVB and UVC are transmitted through the air and quartz but absorbed by glass. UVB radiation can produce skin burns, it is used in the medical field and forensic investigations. Some of their applications are phototherapy, DNA analysis, paint curing or animal treatment to favour vitamin D production.

UVC is more energetic and harmful, used as a disinfection tool which can be split up depending on the medium: air, water or surfaces. UVC radiation can be used to disinfect the air in HVAC (Heating-Ventilation-Air Conditioning) systems and to prevent mould in the cooling coils. Water disinfection is used to purify sewage, drinking water, water subject to industrial processes, and swimming pools as a method that does not pollute the water, far from the case of chemical treatments. Surface disinfection is requested in industries and hospitals to prevent the propagation of diseases and an early deterioration of aliments.

VUV is not commonly used because it needs vacuum to propagate since it is rapidly absorbed by air, that is why it is named “vacuum ultraviolet radiation” and is of no interest in disinfection applications.

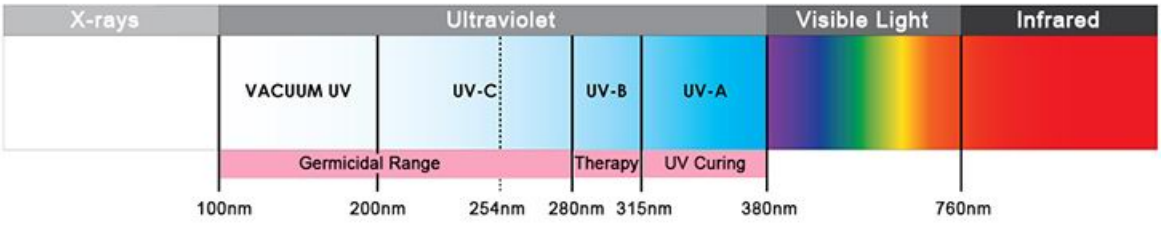

Figure 2.4: Ultraviolet bands position in the electromagnetic spectrum [19].

Ultraviolet radiation sources may be natural or artificial. Natural UV emitters are the stars, such as the sun, and artificial sources are man-made lamps as discharge lamps, incandescent lamps, lasers or LEDs.

The use of discharge lamps is extended to many areas including disinfection applications. Its light is produced by the excitation of a gas sealed in a bulb with two electrodes, and the output spectrum depends on the specific gas and pressure inside the bulb [20] [21]. The mercury lamp offers a broad spectrum between 185 to 2000 nm. It presents intensity fluctuations and an initial period of emission intensity stabilisation (1-15 minutes) [22].

Nowadays, the most common lamps are the low pressure mercury vapor lamps, which produce a discontinuous spectrum with narrow peaks with more than 90% of the spectral power emitted at 253.7 nm. On the other hand, the ordinary mercury fluorescent lamps emit visible light, safe for humans exposure, because the ultraviolet radiation at 253.7 nm activates phosphor fluorescence and the glass tube blocks the ultraviolet radiation. Instead, if the tubes do not contain phosphor and are made of fused quartz, then the lamp is a UVC power source [23].

2.2 Radiation-matter interaction

Maxwell's equations are used to describe the generation of electric and magnetic fields from matter, but when it comes to study the effects of these fields on the matter, that is the radiation-matter interaction. The Lorentz model is used to describe the response of materials to exciting electromagnetic radiation by modelling their atoms as composed by a heavy nucleus surrounded by a cloud of electrons.

The interaction of radiation with matter depends on the optical properties of each material and definitely on the electromagnetic range of study. This interaction is related to the most important optical parameter of materials, their refractive index (n) or their permittivity (ε), which will determine the behaviour of electromagnetic radiation regarding reflection, refraction, absorption or scattering.

The complex dielectric function or permittivity, (ε), is described in the Lorentz model by modeling interband electron transitions [24] with a simple toy-model like a spring and it is

given by

$$\widetilde{\varepsilon}(\omega) = 1 + \sum_{j=1} \frac{f_j \cdot \omega_{0,j}^2}{\omega_{0,j}^2 - \omega^2 - i \cdot \omega \cdot \gamma_j} \tag{2.20}$$

where in the general term j corresponding to the j^{th} resonance, f_j is the resonance strength (related to the quantum parameter "oscillator strength") and $\omega_{0,j}$ its frequency, ω is the frequency of the incident radiation, and γ_j represents the damping constant of the j^{th} resonance.

The relation between complex permittivity and the real and imaginary parts of the refractive index is shown in *Eq.* (2.21). n corresponds to the real part of the refractive index, and κ is the imaginary part, also known as the extinction coefficient, which indicates the amount of attenuation when the electromagnetic wave propagates through the material, so the extinction coefficient is related to the absorption.

$$\widetilde{\varepsilon}(\omega) = (n + i \cdot \kappa)^2 = \underbrace{n^2 - \kappa^2}_{\varepsilon_r} - i \cdot \underbrace{2 \cdot n \cdot \kappa}_{\varepsilon_i} \tag{2.21}$$

The incident frequency is a function of the wave vector, k, and the phase velocity of the wave, v, or simplified, a function of the wavelength, λ, (see *Eq.* (2.22)), hence, the permittivity will change with it, giving rise to different material response according to the range of the incident electromagnetic radiation.

$$\omega = \underbrace{\frac{2 \cdot \pi \cdot n}{\lambda}}_{k} \underbrace{\frac{c}{n}}_{v} \tag{2.22}$$

In *Eq.* (2.20) the resonant frequencies of the oscillator ($\omega_{0,j}$) vary for each material, and when the incident frequency is equal to one of these frequencies, $\omega \approx \omega_{0,j}$, the imaginary part on, k, shows an absorption peak. For very high values of ω (low values of λ and consequently, high values of photon energy) $\widetilde{\varepsilon}(\omega)$ will tend to one, meaning most material will be transparent to radiation. If we focus on a small range of the radiation spectrum, as usually happens in real experiments, *Eq.* (2.20) can be simplified with just one resonance frequency as follows

$$\widetilde{\varepsilon}(\omega) = C + \frac{f \cdot \omega_0^2}{\omega_0^2 - \omega^2 - i \cdot \omega \cdot \gamma} \tag{2.23}$$

where C is a constant parameter involving the influence of neighbour resonances.

Eq. (2.23) can be separated into two parts, $\widetilde{\varepsilon} = \varepsilon_r + i \cdot \varepsilon_i$, the real part associated to dispersion and the imaginary part to absorption. The imaginary part (see *Eq.* (2.25) below) is often referred as a "Lorentzian" because is a weak function of frequency far from the resonance, but near the resonance this function increases sharply to a maximum [25].

$$\widetilde{\varepsilon}(\omega) = 1 + \frac{f \cdot \omega_0^2 \cdot \left(\left(\omega_0^2 - \omega^2\right) + i \cdot \omega \cdot \gamma\right)}{\left(\omega_0^2 - \omega^2\right)^2 + \omega^2 \gamma^2} \tag{2.24}$$

$$\varepsilon_i = \frac{f \cdot \omega_0^2 \cdot \omega \cdot \gamma}{\left(\omega_0^2 - \omega^2\right)^2 + \omega^2 \gamma^2} \tag{2.25}$$

In our case, we will focus on the UV range where, for nucleic acids, the resonance frequency, ω_0, corresponds to λ around 260 nm as it can be seen in the absorption spectrum of *Fig. 1.1*. Therefore, the genetic material of living organisms absorbs this radiation, giving the UVC radiation the possibility to serve as a disinfectant tool.

This fact leads us directly to highlight the relevance of **radiological protection** and the materials that are used to protect us from ionizing radiation, which in addition to being invisible to the human eye, is more energetic and more dangerous. In our case, ultraviolet radiation exposures without adequate protection can cause damage and burns on the skin and eyes.

It is important to remark that transparent materials to visible light are not necessarily transparent to other spectral ranges, for example to ultraviolet light. The same applies to all optical characteristics and coefficients of the materials which are a function of the refractive index and this, in turn, to the wavelength.

Some good examples of ultraviolet radiation absorbing materials are glass, metal foils, most kinds of clothing, some plastics and cellulose. These have to be taken into account as security elements, providing shielding against UV exposure. Moreover, materials transparent to UV are also necessary for UV usage. Such is the case of lamp tubes, which need a material to encapsulate gas while allowing for UV radiation to get through it, as for example quartz glass.

Air interaction is as well relevant because ozone can be produced at wavelengths below 240 nm, but not all UV-C lamps produce ozone. The ozone, O_3, is an unstable gas whose molecules are able to create hydroxyl radicals during its decay to oxygen, which has antimicrobial and oxidizing effects, and in addition, can affect respiratory and nervous systems of living organisms, so the exposure limits are highly regulated.

Ozone can be generated by a combination of methane and fuel combustion products, by short ultraviolet wavelengths (see *Eq.* (2.26) [26]) or in electric discharges containing oxygen. Besides, ozone generation by ultraviolet lamps depends on the radiation power, the humidity, oxygen concentration, temperature and it depends mostly on the wavelength because of the absorption spectrum of molecular oxygen, which has its maximum efficacy around 160 nm.

$$\left.\begin{aligned} O_2 + UV(\lambda < 240\text{nm}) &\rightarrow O + O \\ 2O + 2O_2 &\rightarrow 2O_3 \end{aligned}\right\} 3O_2 + UV(\lambda < 240\text{nm}) \rightarrow 2O_3 \tag{2.26}$$

Besides, ultraviolet radiation can also decompose the ozone due to the absorption peak around 254 nm (see *Eq.* (2.27)) [27].

$$\left.\begin{aligned} O_3 + UV(\lambda < 325\text{nm}) &\rightarrow O + O_2 \\ O + O_3 &\rightarrow 2O_2 \end{aligned}\right\} 2O_3 + UV(\lambda < 325\text{nm}) \rightarrow 3O_2 \tag{2.27}$$

Even though low pressure mercury vapor lamps can emit wavelengths below 240 nm, in general, the lamps' envelope attenuates those emission wavelengths, but some other lamps can generate ozone. Hence, if the manufacturer ensures that the lamps have the appropriate

envelope material, the lamp does not emit ozone, and the odor commonly associated with ozone generation will correspond to the breakdown of organic substances by the 254 nm radiation [28].

2.2.1 Biological medium

Lots of materials are transparent to ultraviolet radiation, however, some materials have their absorption in this range. This is the case of biological material because the electronic transitions of their molecules take place at energies corresponding to that range.

The main interaction between ultraviolet radiation and cells is the absorption by proteins, RNA and DNA. For nucleic acids, the substances which can absorb energy, the chromophores, are the bases; and the photoproducts of the biocidal action of UV are the dimers, formed by the union of two bases. In proteins, the amino acids are the chromophores with an absorption peak around 280 nm which can cause the degradation of the cell contributing to its death, and many organisms have pigments, such as melanin, responsible for absorbing this radiation, so protecting cells. Apart from optical absorption, UV radiation can be scattered by the cells contributing to their photoprotection.

The damage caused by ultraviolet radiation to microorganisms is mainly due to the photochemical changes produced in nucleic acids. Even though all ultraviolet wavelengths being able to cause photochemical effects, the UV-C range is especially harmful to cells because nucleic acids have an absorption peak around 265 nm and proteins can also absorb this radiation [6].

DNA and RNA are translated into the synthesis of proteins, necessary for microbial replication, so damaging these nucleic acids results in the deactivation or the failure to reproduce. The exact process is not completely understood but the interaction with UV radiation produce pyrimidine dimers resulting in multiple transcription errors, protein translation errors and ultimately in the deactivation of bacteria and viruses.

The most common products of the biocidal action of UV radiation are thymine dimers, but in RNA the absorption will be placed in uracil, and other dimers of basis can be found in the case of DNA but each one presents a different degree of absorption because their structure is different (see *Fig. 1.3*). As mercury lamp main emission is at 254 nm, the peak absorption of uracil is closer as can be seen in *Fig. 2.5*.

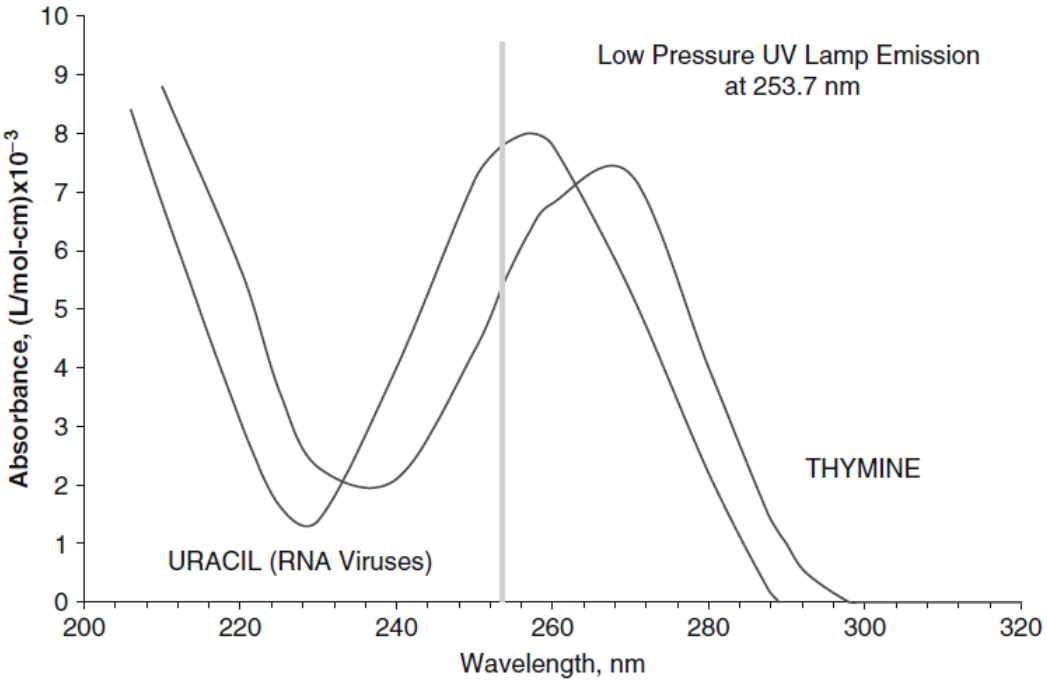

Figure 2.5: Comparison between thymine and uracil UV absorbance spectra[3] as well as the resonance emission of mercury lamps at 253.7 *nm.*

Nevertheless, to deactivate a microorganism is not only necessary to attack the genetic material, but also the biological components responsible for the replication and repair processes, such as the enzymes associated with bacterial cells [3].

Accordingly to the effects produced in live organisms, UV-C is a disinfection tool for bacteria and viruses mostly related to their pyrimidines concentration and not with the size of the microorganisms [6].

2.3 Disinfection methods

Before going deep into disinfection methods, it is pertinent to explain the differences between methods to ensure healthcare safety. Those processes vary according to the product, the organisms, and ambient parameters, consequently, the method depends on the situation, and they should not be mixed up between them.

It is also important to express the efficiency of disinfection processes and in order to do so we can use the log reduction. This mathematical term represents the relative number of microorganisms that are deactivated by disinfection. A 1 log reduction will correspond to the 90% microorganism population deactivated, a 2 log reduction to the 99%, a 3 log to the 99.9% and so on.

According to [4] the **sterilization** implies the elimination of all forms of microbial life,

which in practice is the same as 6 logs or more of rate disinfection. Unfortunately, some health professionals refer to disinfection as sterilization.

Disinfection does not have an absolute definition, it can be described as a process that reduce, inactivate or destroy many pathogenic microorganisms, leaving out bacterial spores on inanimate objects. Disinfection can be carried through chemical processes, as disinfectants, or through physical ones, as heat or ultraviolet light.

On the other hand, the single removal of visible soil from surfaces is known as **cleaning**, which is not enough but it is crucial before high level disinfection and sterilization.

The effectiveness of those methods depends on the type and concentration of microbial contamination, the exposure time to germicide, temperature and the medium in which the microbes are embedded (e.g. "Microbes are more vulnerable in air, whereas microbes on surfaces appear to have a certain degree of inherent protection" [3]).

This work revolves around the concept of disinfection. The role model disinfectant should have a wide range, meaning it should destroy as many pathogenic microorganisms as possible while being fast, efficient and reliable. It is important that the microorganisms do not build resistance in the long term to the disinfection tool. We also want the disinfectant to be harmless to the equipment and objects, nontoxic and free from dangerous residues for people and the environment [29]. Ideally, this disinfectant should be affordable and easy to use, but it is a matter of ease more than a need.

Disinfection can be achieved with different tools such as chemical products (chlorine, hydrogen peroxide, ozone, ...) or by physical methods (heat, UV, plasma...).

In the wide range of disinfectants that exist, chemical cleaners stand out for their varied use, from everyday environments to sanitary environments, such as bleaches or ammonia, which have the disadvantages of releasing toxic gases, being able to cause damage to certain materials and involving personnel in its use. A powerful chemical disinfectant is ozone, used in wastewater treatment and surface disinfection [30]. Ozone is highly efficient against protozoa and viruses, but this technology is complex, expensive and requires ventilation afterward because it is extremely irritating and possibly toxic.

Among the physical disinfection methods, ultraviolet radiation has become the favourite in recent times. Despite the disinfection by UVC can not be carried out with the presence of people, it has a germicidal effect in a wide range of pathogens, concerning every organism that has genetic material. Ultraviolet C radiation does not generate toxic residues, is rapid and does not need consumable products, so the costs are only related to the operational equipment.

2.4 Methods of calculus

In order to analyse how the radiation is distributed into space, the radiation pattern of a light source is studied through ray tracing simulations. Nevertheless, simulations must be

verified with theoretical models, checking that simulations and numerical calculus results are at least of the same order, and as similar as possible. The numerical calculus are based on the physical descriptions exposed in *Section 2.1.1*, in which a tube lamp is considered as infinite points radiating spherically, and the integration along its length allows to know the irradiance on a surface.

2.4.1 Ray tracing simulations

In order to obtain valuable solutions of complex systems, simulations take an essential role in problem analysis, providing the possibility to obtain results and solutions to a defined problem without having the resources and physical spaces, and exploring different configurations in a short range of time.

The chief method of calculus along this work is the ray tracing simulation, which allows to foresee the distribution of radiant energy on surfaces at different distances and orientations with respect to the light source.

In particular, the program used throughout this thesis is the commercial optical design software Photopia (LTI Optics, LLC, Westminster, United States) which is based on ray tracing and simulates the electromagnetic radiation emitted from a source as a large number of rays [31].

The essence of raytracing is to simulate the behaviour of a large set of rays to describe the energy distribution by considering radiation matter interactions such as reflection, refraction and transmission. The ray tracing uses the Monte Carlo method, a probabilistic method that evaluates the optical properties of the materials and radiation sources to recreate real situations.

In spite of Photopia being a software developed for the analysis in the visible range, the basic physic processes can be applied to the ultraviolet range of the electromagnetic spectrum because it does not give consideration of the wavelength. Photopia does not calculate the radiation-matter interaction for a specific wavelength or an amount of them, but permits the user to change the optical parameter of each material, giving the pattern radiation distribution of the wavelength in what the specific lamp under study has its maximum irradiance.

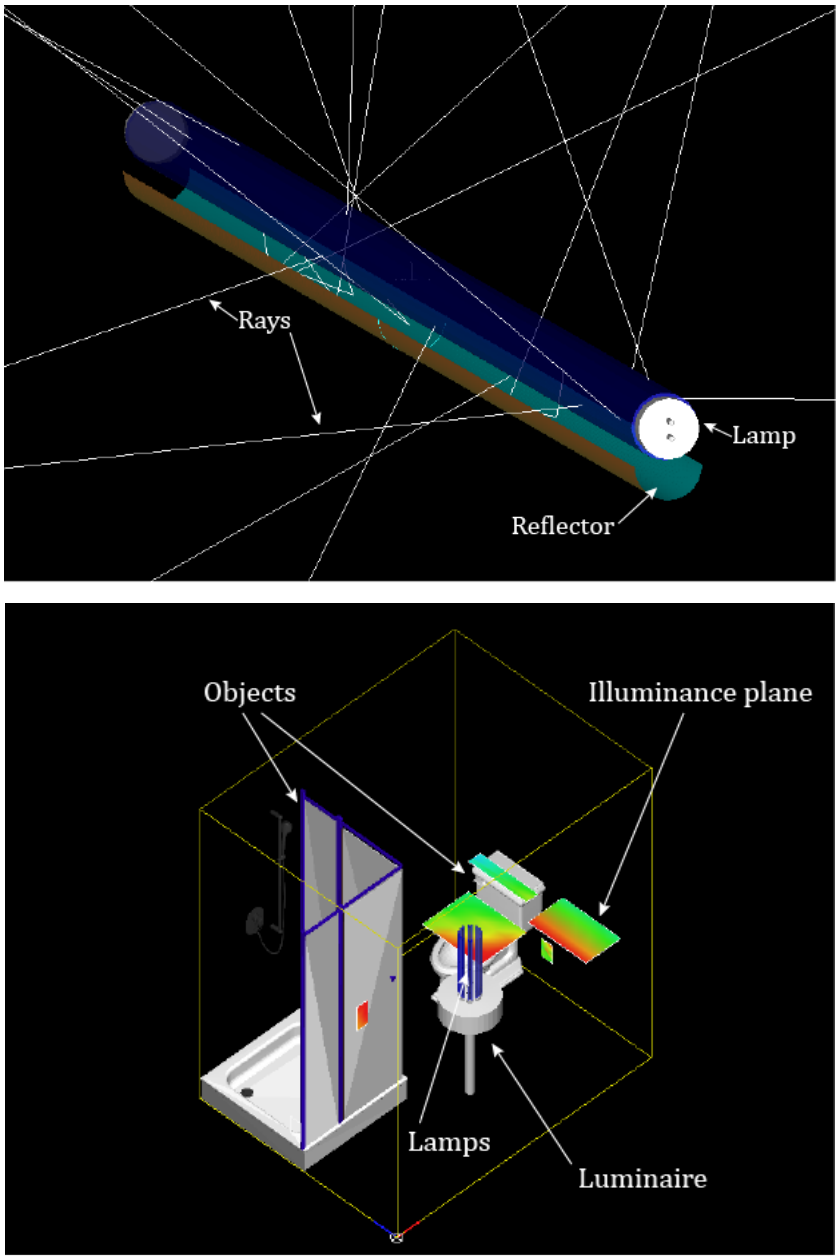

Figure 2.6: View of elements used in simulation in the software Photopia.

The common units used in the visible range are the photometric units, which is the default system of Photopia, but they can be changed to radiometric units to work in the rest of the spectrum to simulate the spatial distribution of radiant energy of UVC systems. Owed to the lack of wavelength used, the main parameter to characterise a lamp will be the flux energy measured in radiant watts, which can be modified to be close to the experimental measurement of the irradiance of the lamp in the wavelength of study.

This program not only has a lamp data base, but includes a built-in CAD (Computer Aided Design) system to design 3 dimensional objects with reflective, refractive and transmis-

sive properties and better recreate real elements as lamp reflectors which take an important role in the location and direction of the rays.

The software gives the possibility to change irradiance parameters of lamps, the coefficients of reflection, refraction and transmission of materials, and the number of rays, which have to be a number between 20 to 50 million rays to have a good resolution model.

The elements that show the irradiance in a region of the space are the illuminance planes, planes created by the user with a specific rectangular size, in a position and orientation of interest. Those planes have a face that is capable to detect the amount of rays that cross their surface, but not the other face which is non interacting. The resolution of sign data in illuminance planes clearly depends on the number of rays emitted by the radiant source, but it can also be changed by the grid density of these planes since the irradiance registered in the illuminance plane is a sum of the rays divided by the bin area. The grid density in a plane or the size of the rows and columns of the grid can be modified by the user, depending on different conditions as the total size of the plane and the distance to the light source.

This simulation program was also used for ultraviolet analysis in [32] [33],[34] and [35], with the intention of predicting the fluence rate fields in the ultraviolet range verifying experimental measurements and numerical calculus. Here can be emphasised the need for direct measurements, for example with a radiometer, to validate the simulation model.

In this work, the software Photopia was used to study some low pressure mercury vapor lamps, which have an irradiance peak in 254 nm. Comparing and adjusting simulation results with numerical calculus and experimental measurements (with a radiometer for UV-C range and 254 nm chemical dosimeters), the lamps were characterised and serve to predict the radiant pattern at different distances and to validate its germicidal effect in biological material.

Chapter 3

Radiometric analysis

This chapter deals with the process needed to evaluate the germicidal effect of any ultraviolet C source. Starting with the validation of simulations, and then the simulations of radiation patterns to characterize a lamp, which in turn will serve to calibrate chemical dosimeters.

Ray tracing simulations allow us to evaluate a large number of lamp locations with varied conditions in a matter of minutes without making real measurements or calculus in each point of space. Hence, proved simulations are useful to study the radiometric analysis, they predict the radiation pattern and unexpected solutions which let to understand the results before taking measurements in the real world.

Simulations also serve to characterize light sources, the absorbance of materials, also to make a first check of the germicidal power of ultraviolet C luminaries, the needed number of devices and their position to disinfect every surface in a room. Both simulations and equipment can be monitored and validated using different methods: radiometer, colourimetric test cards and biological indicators.

3.1 Parallelepipedic geometry

To simulate a real space, you only need to measure the dimensions of the room to be recreated in 1:1 scale in the software. Human made structures tend to be parallelepipedic, thus, the design of the space is reduced basically to draw simple geometries formed by straight lines and rectangles.

Photopia has a library of materials and commercial lamps with their radiation pattern and technical data, that can be modified after importing them. The luminaires, their reflectors and walls of a room can be created with the 3D CAD system of the software. Moreover, some prefabricated objects that can be found on the internet can be imported to the software, with the possibility of changing the size and the surface material properties such as reflectance, refractive index and transmittance.

The software simulates the raytracing in terms of power and trajectory without taking into account the wavelength of the radiation emitted by the source, meaning that the way

to work in a specific range of the spectrum is governed by the properties of materials. Although Photopia was first intended for the visible range, this lack of wavelength use allows us to utilise it for ultraviolet range. Even though the results would be far from the reality due to not doing multiwavelength studies, our work is not affected too much since ultraviolet disinfection sources have a major emission peak (mercury vapor lamps emit a discontinuous spectrum with a main peak at 253.7 nm, see *Fig. 3.5*).

Presence of objects and their orientation

For the purpose of disinfecting every surface of a room, the objects in it and the shadowed areas created by them could be a problem to overcome. Radiation is delivered directly and indirectly thanks to reflection with materials. Varying the irradiation time, intensity and reflectivity of materials, the wanted level of disinfection could be achieved, including some shadowed regions due to indirect irradiation.

After fixing the properties of the lamp and the materials of a room, the radiation pattern will not be only a function of distance, but the surface orientation will be also relevant. Mathematically, it is easy to see that orientation has a more relevant role than the distance (see *Eq.* (2.14) and *Eq.* (2.18)) because the irradiance is proportional to the cosine of the angle between the normal of the object and the ray trajectory. Nevertheless, this fact is not intuitive, so simulations results can help to understand it in a visual manner, as it can be shown in *Fig. 3.1*.

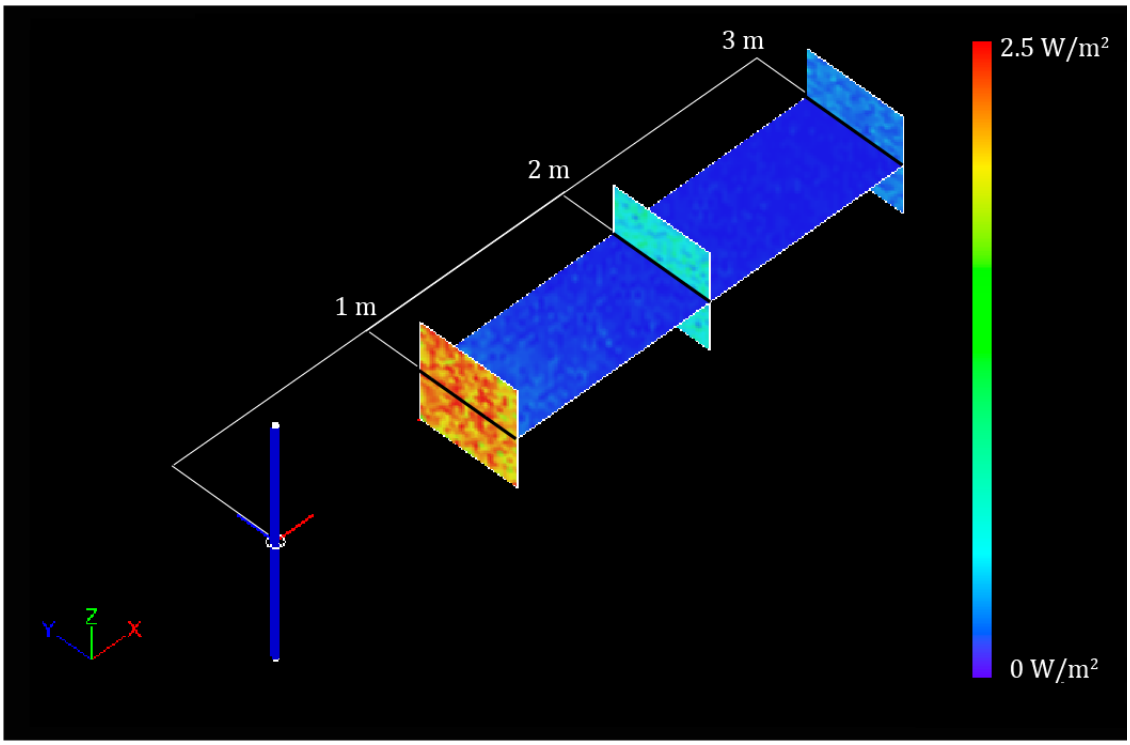

Figure 3.1: Irradiance comparison at the same distance to the source with different orientation surfaces. All the illuminance planes are in the same colour scale which is shown in the right side of this figure.

As irradiance can be calculated in one point, a set of points calculus can recreate a surface; however, the results would not be correct unless the orientation of the surface was taken into account. This detail is shown in *Fig. 3.1*, where the same line (painted in black) registers different irradiation values depending on the orientation of the surface to which corresponds.

Irradiance contours of those planes of *Fig. 3.1* are shown in *Fig. 3.2* to compare the results along the same line. The black rectangles in *Fig. 3.2* delimit the region of interest, which corresponds with the black lines of *Fig. 3.1* to see the difference of irradiance due to the orientation of the plane with respect to the light source.

Fig. 3.2 shows the attenuation of radiation through space. Moreover, irradiation results can be compared in the same point of the space but in horizontal and vertical planes. It can be seen how vertical planes receive more radiation than the horizontal ones despite being at the same distance.

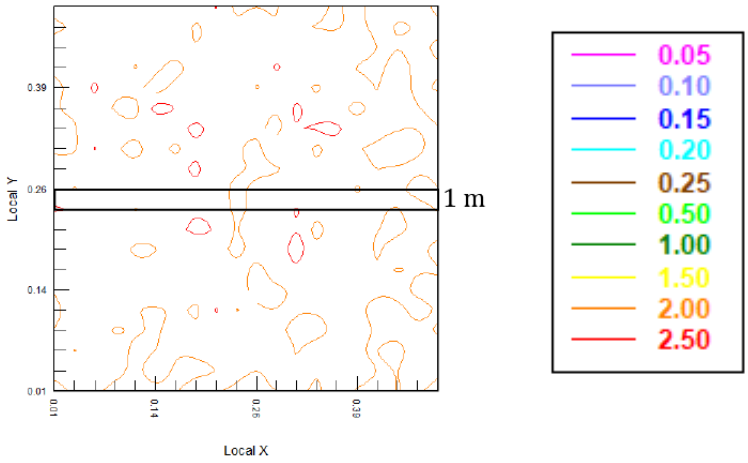

(a) Vertical illuminance plane at 1 m and the colour scale of all the contours of these plots.

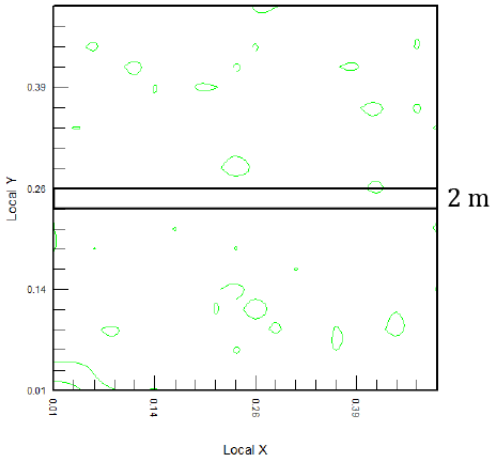

(b) Vertical illuminance plane at 2 m.

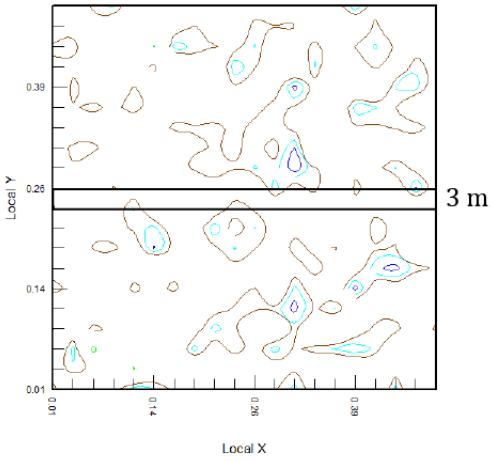

(c) Vertical illuminance plane at 3 m.

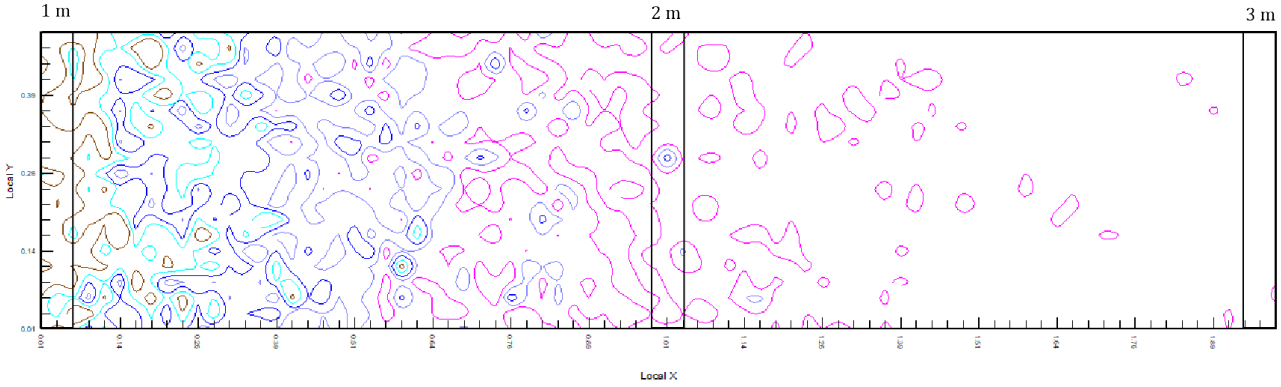

(d) Horizontal illuminance plane.

Figure 3.2: Irradiance contours in the illuminance planes of Fig. 3.1. All of them have the same colour scale in order to facilitate its visualization in units of W/m^2.

3.2 Characterization and use of a luminaire

Simulations are used to calculate the radiation pattern, however, the results are useless until the light sources are characterized, meaning that simulation and real source radiation must be compared and verified to be the same. Therefore, to use a luminaire in a radiometric study associating simulated patterns with real results is necessary to characterise the device.

To simulate the luminaire, the same exact lamp (or, if not possible, one with very similar dimensions) is imported from the data base. Taking measurements of the luminaire will help to design reflectors and the skeleton of the device. In order to have the same light source, it is important to check the electrical and radiant power values given by the manufacturer. Once the luminaire is recreated in the simulation environment, the irradiance can be calculated over any surrounding surface by drawing illuminance planes. The irradiance values of those planes must be compared with the results measured with the radiometer in the same positions as the real luminaire. For this work, the radiometer used is a specific sensor of ultraviolet C radiation whose responsivity is shown in *Fig. 3.3*. If the results in several points do not agree between radiometer and simulations, the radiant emission power of each simulated lamp has to be changed until results match, thus obtaining the actual radiant flux emitted by the lamps of the real luminaire.

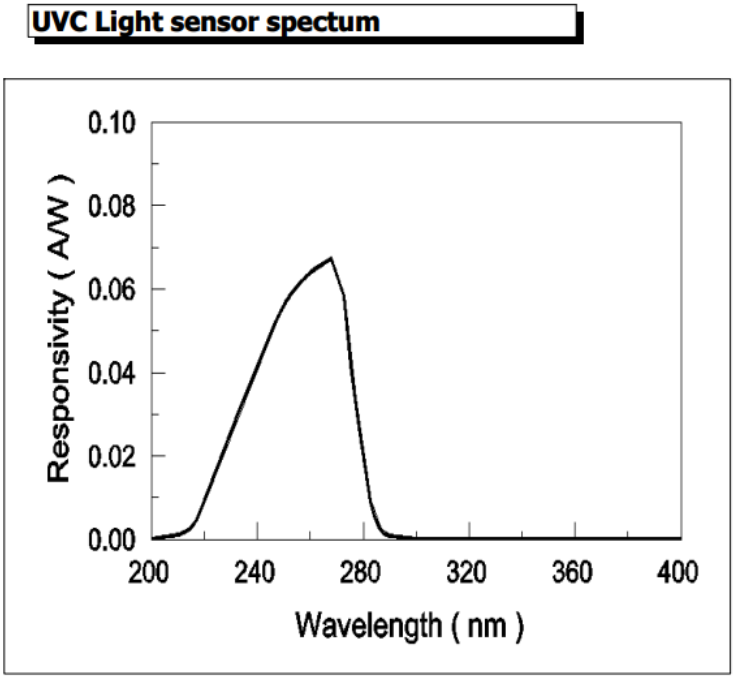

Figure 3.3: Responsivity of the ultraviolet C radiation radiometer [36].

The radiant power data (which in our case is the flux emitted in ultraviolet C range) can be found in some manufacturer's datasheets such as the case of Philips' lamps, but in other cases, it does not even name it, although it is the key data for calculating irradiance, so it will have to be obtained by making a considerable amount of measurements of the real source.

Following with the luminaire simulation, an ultraviolet C radiation luminaire is shown below as an example (see *Fig. 3.4*). This specific luminaire has been used all over this work, to validate simulations, and after being characterised, to radiate samples. It has also been used as a dosimeter calibration source, as will be explained in *Section 3.2.2*.

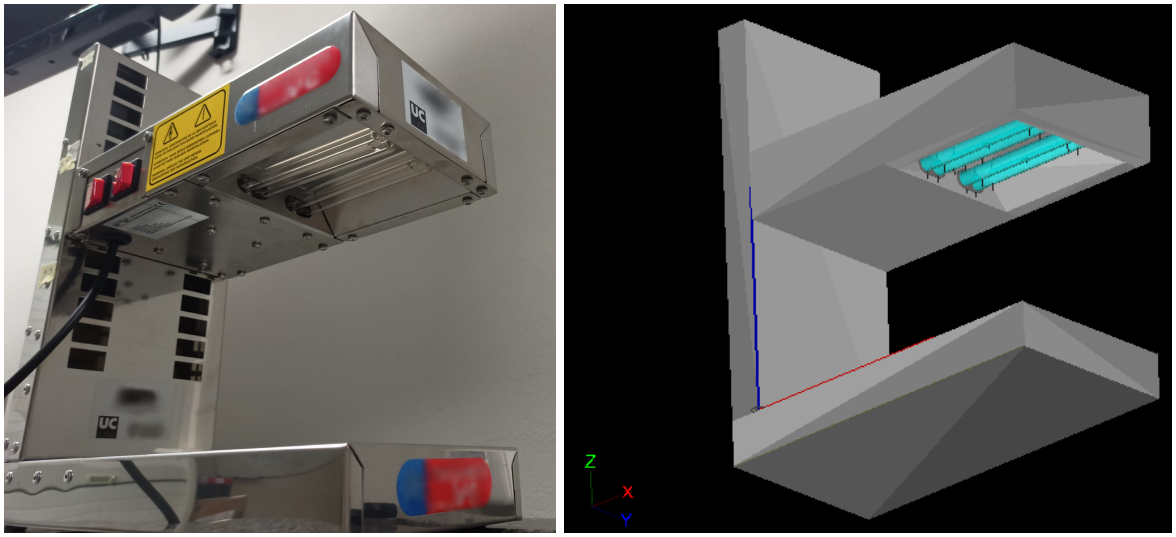

(a) (b)

Figure 3.4: Luminaire a) in real life and b) in Photopia simulation.

The luminaire has a movable part where lamps are located (14 positions available, see Appendix *A*), is composed of two Philips lamps (TUVPL – S9W/2P1CT/6X10BOX) with 9 electrical W, 2.3 radiant W and has its main emission peak around 254 nm which can be seen in *Fig. 3.5*.

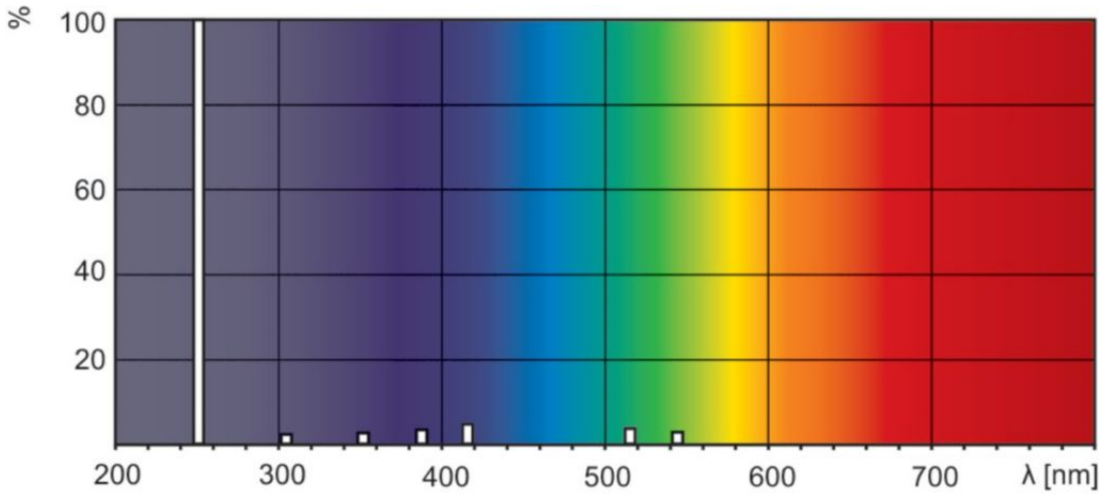

Figure 3.5: Spectral power distribution of the Philips lamp TUV PL-S 9W [37].

In order to carry out the irradiance comparison, the base of the luminaire which was just below the lamps was divided into 12 squares in which the radiometer was located and measurements were taken for three different heights of the lamp case (numerated heights as 4, 9 and 14). So 36 point measurements were used as a reference to characterise the simulation of this specific device, which has been characterized with 1.3 radiant W of ultraviolet C radiation (lower than the 2.3 radiant W given by the manufacturer), and from then on able to obtain the irradiance at any point of the space with any height of the lamp case as if the measurements were taken with the radiometer.

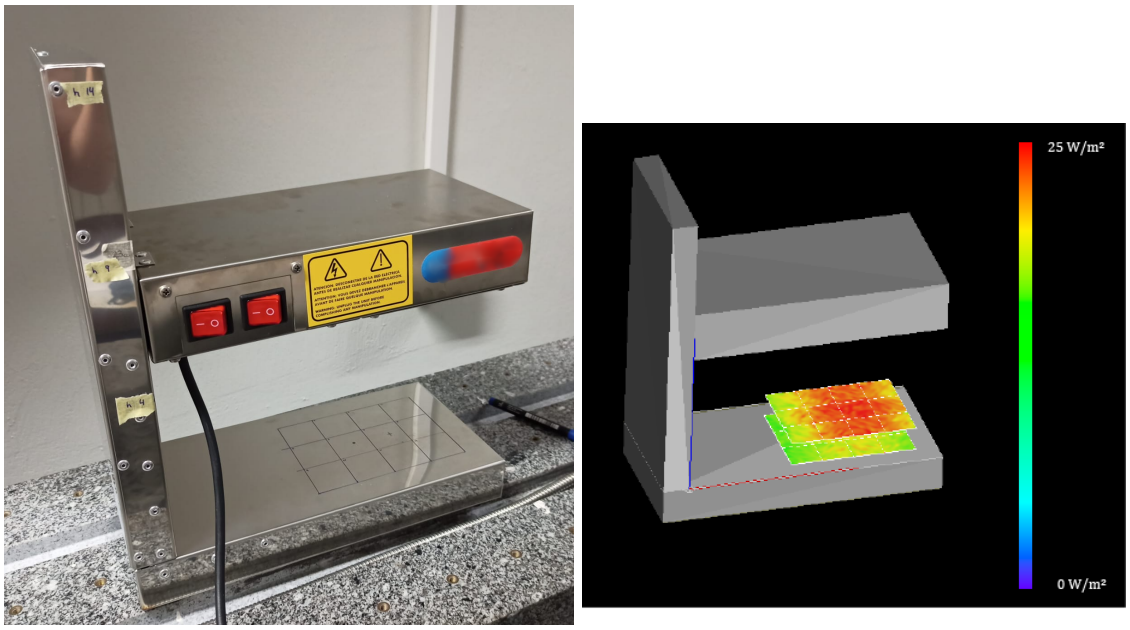

(a) (b)

Figure 3.6: Measurement grid in the ultraviolet C luminaire used in this work, a) in real life and b) in Photopia simulation.

3.2.1 Lamp response

Although the lamp has been characterized and the irradiation of the luminaire at each point in space is known, to calculate the dose it is not enough to multiply the exposure time by the irradiance obtained at a point, since the lamps are not perfect emitters, and they fluctuate. These variations in irradiance over time mean that the dose is defined by the stabilization curve (characteristic of each lamp).

The stabilization curves for 20 minutes are shown below, measuring irradiance in one point every 5 seconds. The curves shown as an example correspond to the central grid (position 7) with the lamps at height 9 of the luminaire. In addition, the temperature of the lamp is measured through a thermocouple in contact with the quartz of the tube lamp.

Fig. 3.7 include lamp measurements of its irradiance and temperature when each lamp is

turned on individually. Those curves are fitted to exponential functions to obtain the accumulated dose for any time within this 20 minutes interval through the integration of the curve.

In *Fig. 3.8* the individual measurements are compared with the other lamp to confirm they can be simulated as the same lamp. It can be seen that they have in practice the same response.

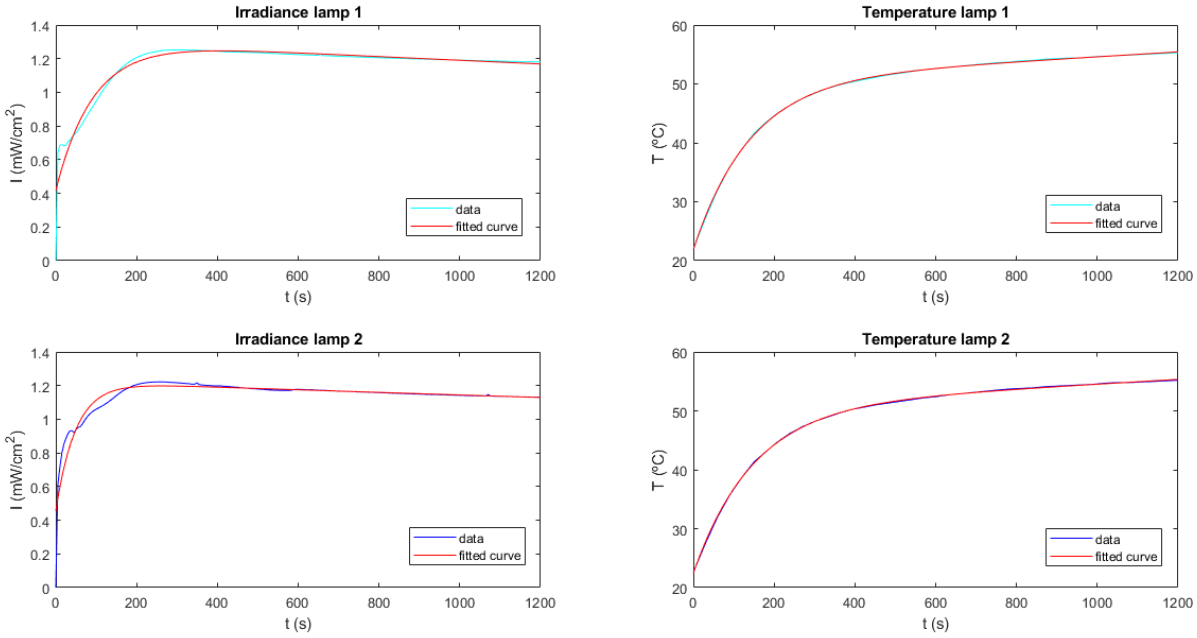

Figure 3.7: Individual irradiation and temperature of the two lamps that compose the luminaire of Fig. 3.4 measured in the base position 7 at the height 9.

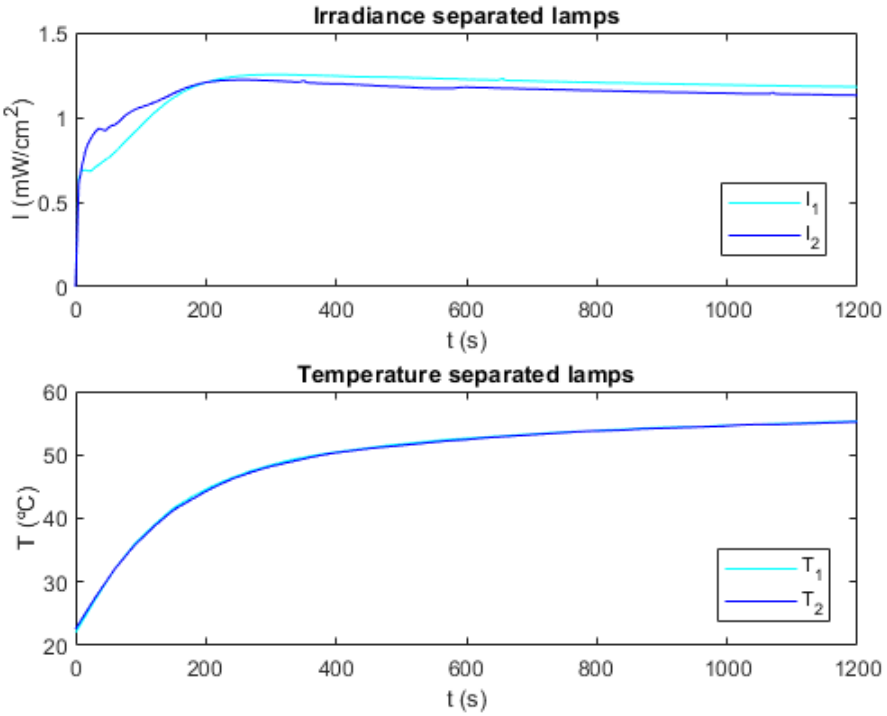

Figure 3.8: Comparison of irradiance and temperature of each lamp working individually.

This same measurement is carried out by turning on both lamps at the same time, and is compared with the sum of individual irradiances. In *Fig. 3.9* can be observed the same maximum, and variations possibly due to the current distribution of the equipment electronics.

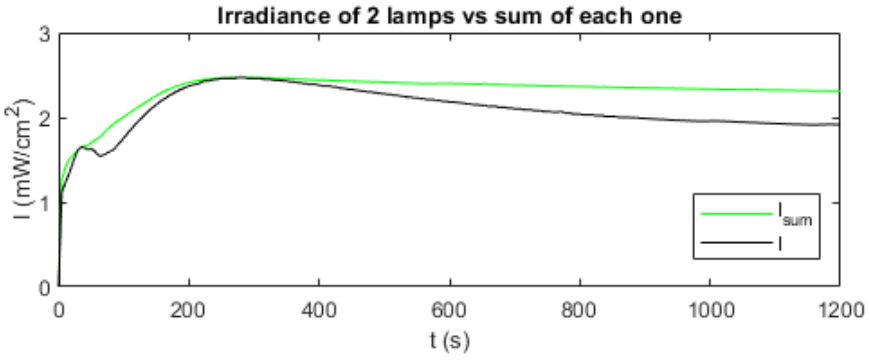

Figure 3.9: Comparison of the irradiation sum of each lamp and the irradiation of the two lamps working at the same time.

These stabilization curves serve as part of the characterization of the equipment regarding its real germicidal effect, obtaining the accumulated dose more precisely by integrating these irradiance curves.

3.2.2 Dosimetry

A dosimeter is any device used to measure the absorbed dose of external radiation. There are different types of dosimeters, such as chemical, electronical and biological. In this section, we are going to explore the chemical dosimeters, in particular, the 254 nm colourimetric ultraviolet indicators from Intellego Technologies, which has the patent of a photochromatic ink that changes its colour to indicate the level of ultraviolet C irradiation.

Those chemical dosimeters are disposable indicators made of a substrate with a photoactive ink that reacts to 254 nm radiation inducing a change in the pH which affects the pigment and changes its colour [38].

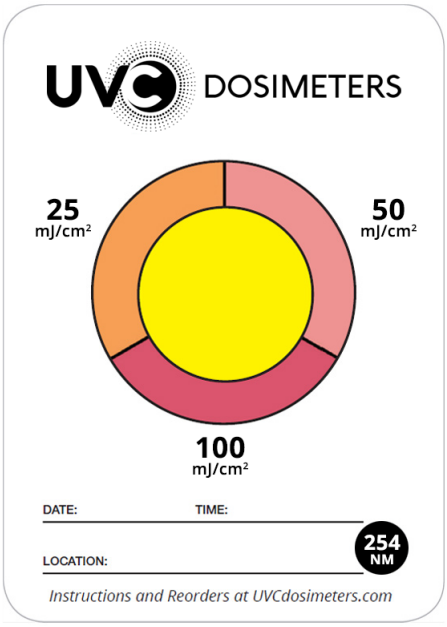

Figure 3.10: UVC 254 nm chemical dosimeter card from Intellego Technologies [39].

Therefore, the indicator changes colour depending on the amount of absorbed dose. The change in colour can be classified in different tones, perceptible for the human eye, associated with cumulative doses, going in a colour scale from yellow to magenta tones associated with doses from 0 to 100 mJ/cm^2 respectively (see *Fig. 3.10*).

Although this colour change can be appreciated by the naked eye, knowing more precisely the absorbed dose is not so easy. For this purpose analogical methods are needed, one way could be spectrophotometry (studying the reflection spectrum and its variations at some wavelengths for different doses), but in this work, we focused the analysis in colourimetric methods as will be shown in this section.

We can use this type of dosimeters to measure the irradiance at different locations during the disinfection of a room. These measurements allow us to be sure that the simulations are correct, and the disinfection process is working properly. Such measurements could be done by a radiometer, but it requires as many radiometers as points you want to register at the

same time, being a radiometer more expensive and less suitable for surface measurements, as the photometer is inside a plastic box which covers part of the incident radiation. Thus, chemical card dosimeters are the most suitable devices to check simulations *in situ* for being cheap, handy and able to correctly measure the incident radiation on a surface.

To be able to relate colour and absorbed dose, we irradiate some of those dosimeters with the characterized luminaire during different exposure times, so each of them gets a different dose and therefore a distinct colour, as shown in *Fig. 3.11*.

Figure 3.11: Chemical dosimeters exposed to doses between 5 to 100 $\mathrm{mJ/cm^2}$ *showing colour tones between yellow and magenta respectively.*

The colour is a light characteristic determined by the spectral composition and the physiological response of the eye, so its perception is subjective. In order to realise the colour-dose calibration in an objective way, a Konica Minolta CR-400 colourimeter has been used [40]. A colourimeter quantifies colours according to coordinates of a colour space by analysing reflectance measurements. Therefore, a colour space is a system that numerically describes a colour into principal characteristics as hue, saturation and brightness or the amount of primary colours.

In our case, the chemical dosimeters are measured within the CIELAB colour space (strictly CIE 1976 $\mathrm{L^*a^*b^*}$) which is represented in *Fig. 3.12*, in which $\mathrm{L^*}$ indicates the brightness with values between 0, corresponding to black, and 100, corresponding to white; $\mathrm{a^*}$ is a chromatic coordinate from the amount of green to the amount of red in the range $[-128, 127)$;

and b* is the same as a* but with the amount of blue and yellow.

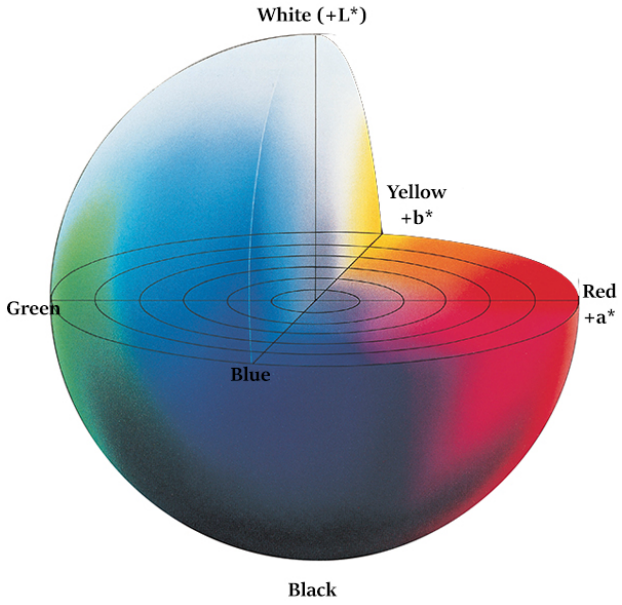

*Figure 3.12: CIE 1976 L*a*b* colour space representation [41].*

After registering the coordinates values of dosimeter colours for different doses, some coordinates changes have been used in order to visualize those colours. CIELAB colour space was transformed to CIEXYZ and then to CIExyY with the only purpose to improve its visualization by representing the colour in 2 dimension space (see *Fig. 3.13*).

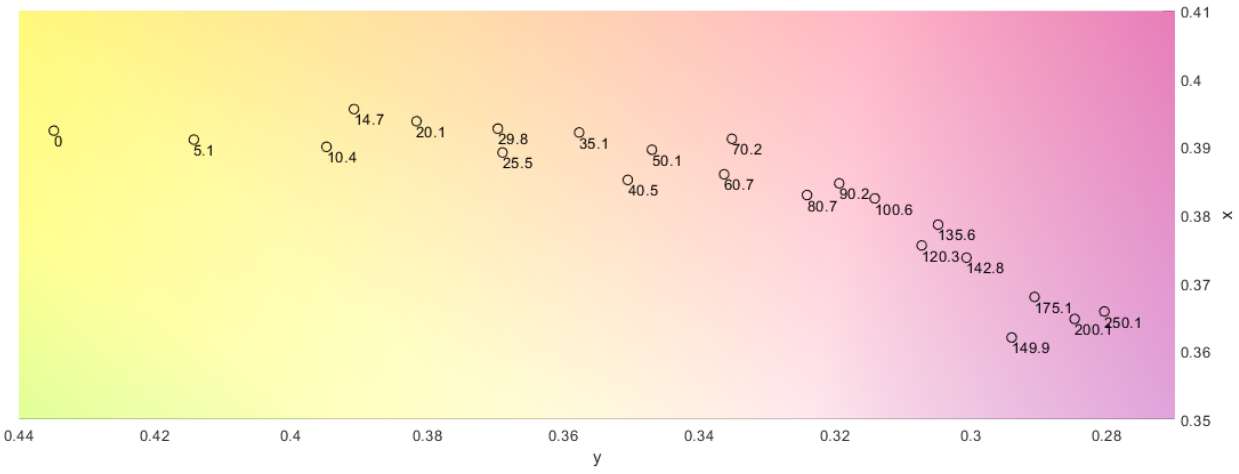

Figure 3.13: Colour diagram (in CIExyY colour space) of measured dosimeters exposed to different radiation (from 0 to 250 $\mathrm{mJ/cm^2}$*).*

Furthermore, to achieve the calibration of chemical dosimeters, we need a function relating colour and dose. For this purpose, we can continue using the CIE 1976 L*a*b* colour space, in particular, the total colour difference parameter [42] [43], which is determined as

$$\Delta E^* = \sqrt{(\Delta L^*)^2 + (\Delta a^*)^2 + (\Delta b^*)^2} \tag{3.1}$$

where this total colour difference ΔE^* corresponds with the distance between the colour we are interested in, and the colour of zero dose.

Intellego cards are specifically designed for a range of ultraviolet C dose between 0 and 100 mJ/cm^2. In this range, we have calibrated the colour difference for different doses, and with the fitted function, we are able to calculate accurately the absorbed dose of any measurement.

In some cases absorbed dose exceeds the upper limit, so we decided to extend the calibration curve up to 250 mJ/cm^2. Although this new calibration range could be less fine than the other one since dosimeters are not designed to work at such doses, it will be used to classify colours from high doses. All these calibration points are shown in *Fig. 3.14*, where the curve is fitted to facilitate the calculus of a specific dose.

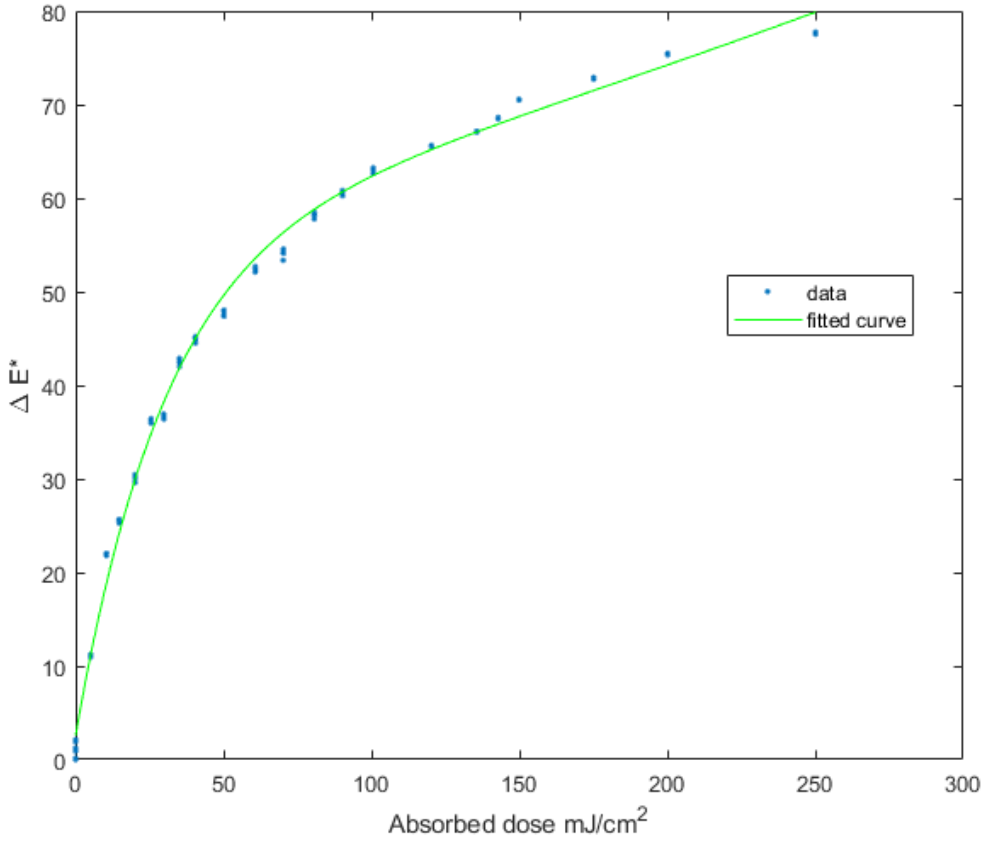

Figure 3.14: Chemical dosimeters calibration. Colour difference as a function of the absorbed dose.

This calibration curve presents an exponential behaviour with a saturation for high doses, which is attributable to the amount of photoactive ink available in the card. Here, the amount of ink was chosen by Intellego in order to have a measurement range between 0 and 100 mJ/cm^2, in which the majority of doses to disinfect a wide range of microorganisms fall down.

On one hand, colourimetric UVC chemical dosimeters have demonstrated their advantages, including the easiness to handle, its specific reaction to the 254 nm radiation, and the measurement precision obtained with the colourimetric analysis. On the other hand, this type of dosimeters present drawbacks such as they only have one use, the colour change is not proportional to colour so a deep analysis is needed, and measurements have to be taken just after the exposition, since its stability post-irradiation depends on the absorbed dose, and heat modifies the initial colour change as time goes by.

Chapter 4

Biodosimetric analysis

At this point, we have the basic knowledge and tools to calibrate UV radiation sources and to use them as a disinfection device. Now, it is time to evaluate the UVC germicidal power.

The biodosimetric analysis pretends to deal with the effect of ultraviolet C radiation on live organisms, and to determine the germicidal effectiveness according to the type of considered microorganism, which is described through mathematical models (*Section 4.1.2*). Although living organisms, such as bacteria, can be used as biodosimeter, DNA samples can be used too. DNA samples are good biodosimeters because ultraviolet C radiation is able to make changes in the living organisms DNA. This is why we used DNA samples to get the results reported in this section.

Along this chapter, we will discuss the effect of ultraviolet C radiation on an in vitro model to assess the damage produced on a short DNA sequence. Independently of the microorganism (virus, bacteria or a human cell), we want to check the DNA damage caused by UVC radiation. To do this, a DNA sequence corresponding to the ODZ1 protein is placed on different substrates and the degree of damage is quantitatively analyzed.

4.1 Microorganism response

4.1.1 UVC disinfection effectiveness

The genetic information of living organisms is encoded in DNA and RNA nucleic acids, which usually reside in the nucleus of eukaryote cells, in the nucleoid of prokaryote cells (such as bacteria) or covered by a protein shell as in the case of viruses.

In living organisms, each basic piece of nucleic acids, the nucleotides, are the main absorbers of ultraviolet C radiation above 230 nm, and the proteins are the principal absorber component of radiations with wavelengths below 230 nm [44]. Furthermore, when a microorganism is radiated with UVC, the doses to denature proteins are higher than those needed to inflict damage on nucleotides, thus, the inactivation of microorganisms depends on the UV absorption by nucleotides, which triggers a photochemical reaction: the formation of dimers between two adjacent nucleotides.

The dimers formation disrupts the nucleic acids structure, causing failures that may make impossible its replication. This results in deactivation, which is the basis of disinfection.

The pathogen susceptibility to UV light depends on the microorganism and the medium where it is embedded. In general, microorganisms are more susceptible in air than in water or on surfaces. According to [44] not all the pathogens show the same sensitivity to UVC radiation, *Fig. 4.1* ranks them considering their sensitivity in air and on surfaces:

$$bacteria \approx protozoa > most\ \ viruses > bacteria\ \ spores > adenovirus > algae$$

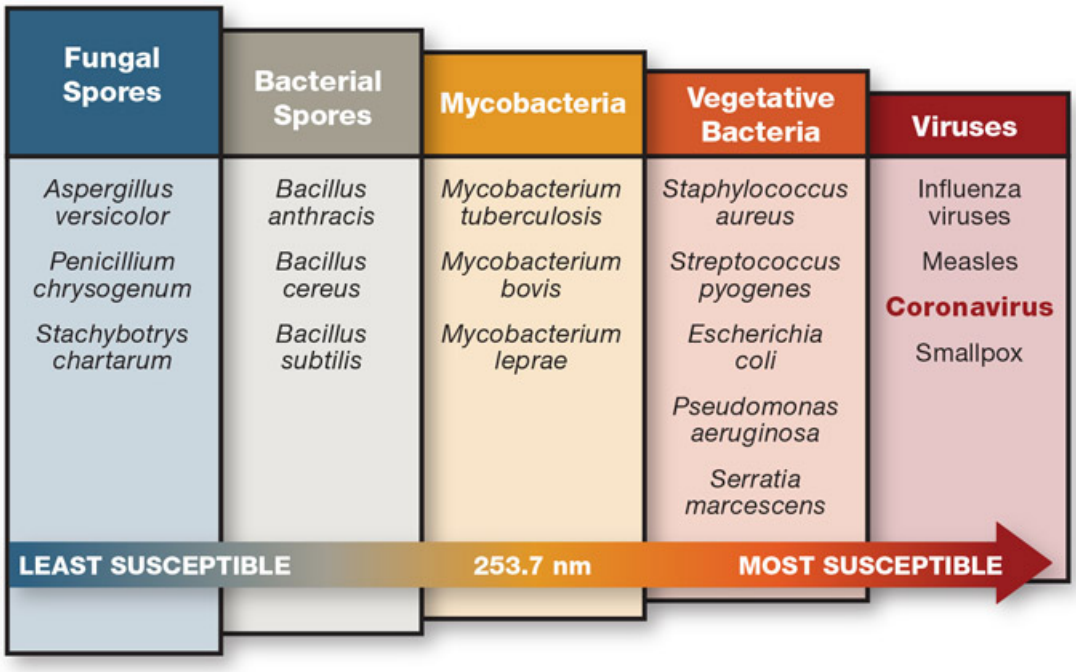

Figure 4.1: Microorganisms susceptibility to germicidal UV-C [45][46].

The ranking shown in *Fig. 4.1* is only a general guide that should not be taken literally, since each group of microorganisms is made up of a variety of species with different susceptibilities. In the case of viruses, the range of susceptibilities is even broader than for bacteria or fungi [46]. This fact can give a justification of why some authors as [3] say that on average viruses are more resistant to UV inactivation than bacteria.

Bacteria and viruses are more susceptible in the air than on surfaces or within water [3]. In addition to the type of microorganisms and the medium in which they are, humidity and thermal conditions are involved together on the photoprotection effects and repair mechanisms of the microorganisms.

Photoprotection of nucleic acids is often related to external shells and absorbent pigments which absorb part of the UVC radiation, reducing the amount of radiation that reaches the

genetic material, which can have different degrees of packaging, leaving more nucleotides exposed to radiation or not.

Damages produced from UVC radiation can be repaired as certain microorganisms have photorepair mechanisms, which will be useless if the received dose is increased [47].

Reactivation mechanisms

The reactivation mechanisms can be divided into two, dark and light mechanisms, referring to those which do not require light activation and those which do, respectively [44]. Reactivation mechanisms are most common in bacteria.

Dark reactivation mechanisms: the caused damages in DNA can be repaired by replacing the sequence of adjacent nucleotides to the dimer created by the absorption of UV with the corresponding sequence. Another possibility is the replication of undamaged regions and the reconstruction of DNA identical to the original, as the same information is coded in the two strands of the double helix, so both strands contribute with their undamaged regions.

Light mechanisms also named **photoreactivation** need near UV and short-wavelength visible light. The prevalent mechanism is the photoenzymatic repair, consisting of the activation of photolase enzyme with light, which is able to restore the original DNA by splitting the dimers [44].

All in all, in order to deactivate a microorganism, the main target is the genetic material, but damaging the components responsible for repair mechanisms can be also helpful to prevent the reactivation.

4.1.2 Mathematical models

This section explains how the germicidal effect of radiation on complex living microorganisms is mathematically modelled for illustrative purposes.

The germicidal effect depends on the received dose, which was defined in *Chapter 2* as

$$D = E_e \cdot t \tag{4.1}$$

where D is the radiant exposure or dose ($\mathrm{J/m^2}$), E_e is the irradiance ($\mathrm{W/m^2}$) and t is the exposure time (s).

In order to quantify the germicidal effect on each type of microorganism we can calculate the survival fraction S by using an exponential decay model [46],

$$S = \frac{N}{N_0} = e^{-k \cdot D} \tag{4.2}$$

where N is the concentration of microorganisms after exposure to UV light, N_0 is the concentration of microorganisms before exposure to UV light, k is the species-dependent inactivation

rate constant and D is the absorbed dose [47].

An improvement of this model takes into account that usually a tiny fraction of the microbial population exhibits a higher level of resistance to disinfection, therefore, the survival fraction can be better modelled as a two stage decay,

$$S = (1 - f) \cdot e^{-k_1 \cdot D} + f \cdot e^{-k_2 \cdot D} \tag{4.3}$$

where k_1 and k_2 are the rate constants associated with each stage and f is the fraction of the microorganism population that exhibits a higher level of resistance to UV radiation. This two stages model is shown in *Fig. 4.2*.

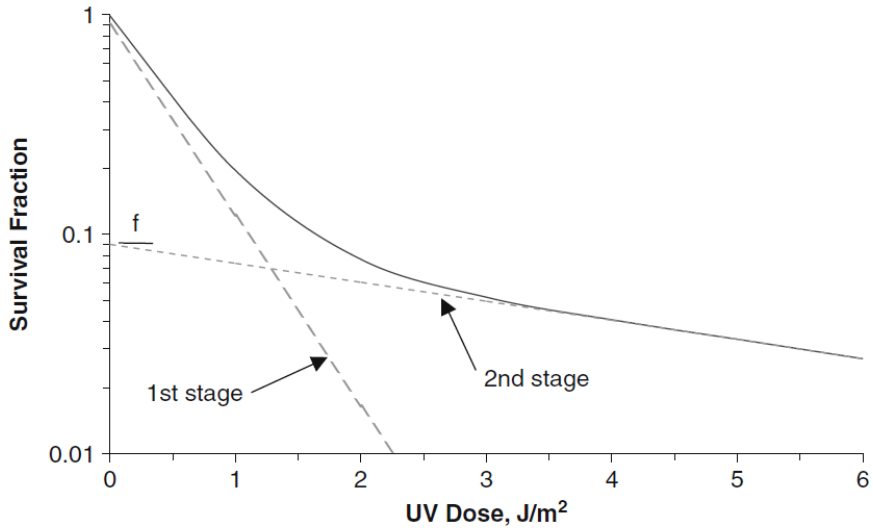

Figure 4.2: Representation of the survival fraction in a two stage decay model [3].

The survival fraction information is usually expressed as another common parameter, the D_{90} value, which corresponds to the dose required to deactivate the 90% of the microorganisms sample, that is, 10% survival. D_{99} is also usual, is used to indicate the dose that results in a 99% inactivation [3].

4.2 Protocol of samples

The definition and role of dosimeters has been shown in *Section 3.2.2*, specifically the chemical ones, however, we are going to focus on biological dosimeters to validate the germicidal efficacy of UVC sources. In order to test the germicidal effect of an ultraviolet radiation device, it is not enough to know the dose that reaches each point in the space, but we must assess the damage it causes to biological material.

Each type of microorganism has different characteristics, therefore the method to use a microorganism as a dosimeter and the analysis of the damage it suffers will not be always

the same. For instance, one method would consist in spreading a fixed number of bacteria onto nutrient agar, then exposing them to UVC radiation, after which the sample is left in a favorable environment for the growth of bacteria colonies and finally, after 24-48 hours the number of colonies is counted. Another example is the study on viruses, which is performed with samples of their genetic material, and the analysis is carried out by means of the PCR (Polymerase Chain Reaction) technique to examine DNA damage.

Since both, the motivation for this work and the development of UVC devices, come from the current COVID-19 pandemic, the process for preparing and analyzing the damage produced by UVC radiation in a specific plasmid of 1500 base pairs (bp) of an ODZ1 gene will be explained below.

4.2.1 DNA sample preparation

For the purpose of preparing a DNA biodosimeter, we use a commercial gene and we perform a PCR process on it in order to increase the number of double strands of genetic material. In addition to the original DNA sample, some other components are needed to amplify it by the PCR process, each of them takes an important role and they are added in the following proportion: 1 μg of DNA, 0.5 μl of dNTPs 2 mM (from Sigma), 1 μl of GLP1 and 1 μl of GLP2 (both 10 μM of concentration, from Metabion), 0.25 μl of taq polymerase (from Kapa Biosystems), 5 μl of buffer 10X (from Kapa Biosystems) and 31.75 μl of distilled water.

The PCR is a molecular biology technique whose goal is to obtain a great amount of copies of a DNA fragment. The DNA sample contains the target sequence to amplify. The dNTPs are nucleotides that serve to build new DNA chains. GLP1 and GLP2 are the primers (forward and reverse), those are short segments of nucleotides complementary to a section of the DNA sample. Each one of those primers is designed to join to the start (forward primer) and end (reverse primer) of the sequence which is going to be amplified [48]. Taq polymerase is a thermally stable enzyme responsible for the duplication of DNA, and the buffer is the medium in charge of maintaining a stable pH and ensure the proper DNA synthesis function of the polymerase during the PCR. A TE buffer solution is used to solubilise DNA while protecting it from degradation.

The PCR is done in a thermocycler (from Applied Biosystems), a device capable of performing temperature cycles necessary for a DNA amplification polymerase chain reaction. This process consists of three steps: denaturation, annealing and extension; which are represented in *Fig. 4.3*. First, the **denaturation** to split the DNA double helix into two chains by a process of heating, then, the **annealing** or primer binding to the DNA strands, and finally the **extension** which consist in the synthesis of new DNA by detecting the primer and transcribing the specific gen [48].

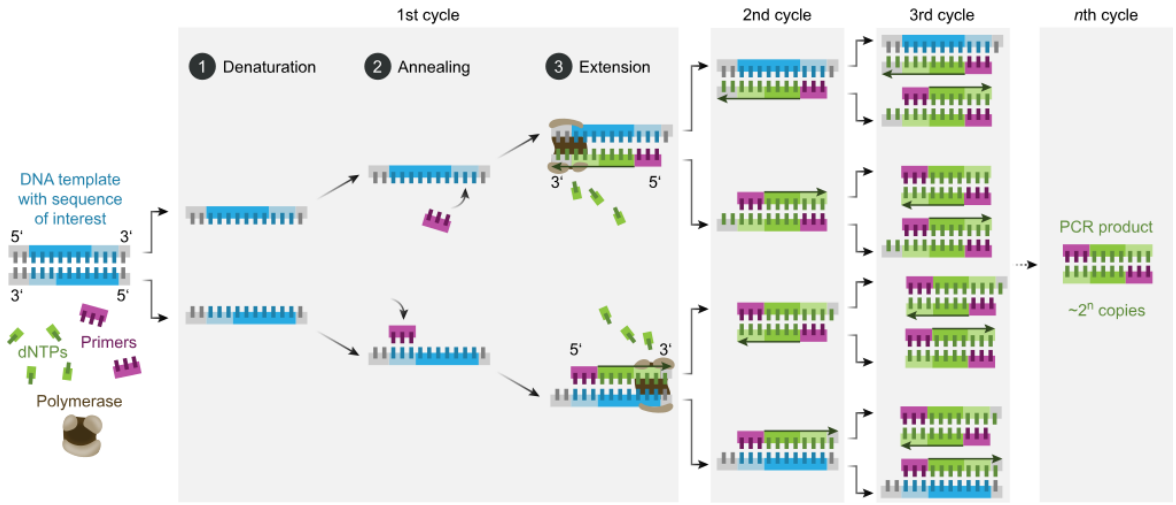

Figure 4.3: Steps of Polymerase Chain Reaction [49].

In our case, the process begins with 4 minutes at 94°C to separate the strands, then 20 cycles of 30 second each one at 94°C in which primers join to the chain and 5 minutes at 65°C for the elongation. After these 20 cycles, 10 minutes at 73°C are needed to bind the strands, and to conclude, the sample is kept at 4°C.

As a result of PCR, and after sample purification, we have multiple DNA chains. After that, we make a quantification to know the amount of DNA per unit volume. For this quantification, a Qubit 3.0 fluorometer is first calibrated with two calibration samples (containing buffer, a standard and a fluorophore from Realsafe) and then, used for measuring our own sample (containing buffer, a fluorophore and the purified DNA). The result of the quantification was 42.1 ng/μl, so, in order to obtain a droplet with 100 ng of DNA, we need 2.4 μl of this analysed sample.

4.2.2 Irradiation, analysis and germicidal effect on ODZ1

We made three types of biodosimeters, each one of them composed of a droplet of 2.4 μl. Two of them use parafilm as substrate. In one case, we use a wet droplet and in other case we let it dry. The last type of biodosimeter consists of a dry droplet on a whatman paper. The different conditions given by each type of dosimeter will be reflected in the DNA damage results.

Following that, biodosimeters were exposed to UVC radiation in our calibrated luminaire, therefore the received dose is known and controlled with the exposure time. We make 6 dosimeters of each one of the 3 types, to expose them to different doses and observe the effect produced on the DNA. One sample acts as a control, so it will not be exposed to radiation, and the rest will receive doses equal to 5 mJ/cm^2, 15 mJ/cm^2, 30 mJ/cm^2, 60 mJ/cm^2, and 120 mJ/cm^2 (the required times are shown in Appendix B). After that, the sample is removed from the support with 50 μl of TE buffer in an eppendorf tube, mixed in a vortexer, recovered by pipetting and stored in freezer.

The analysis is done by a PCR, because this process does not only serve to amplify a sample, but it can determine the degree of damage suffered by the template DNA, because PCR needs relatively intact DNA to perform an efficient amplification. Therefore PCR is able to detect damages on DNA, not only dimers, but also broader types of damages that prevent the replication of genetic material, making it non amplifiable [50].

The **results of DNA damage** can be analysed by a quantification carried through a fluorometer, or by image analysis with a transilluminator.

The quantification is done with the Qubit 3.0 fluorometer, in the same way as the previous quantification, obtaining the results of *Table 4.1* which are represented in *Fig. 4.4*.

ng/μl	Control	5 mJ/cm^2	15 mJ/cm^2	30 mJ/cm^2	60 mJ/cm^2	120 mJ/cm^2
Wet droplet on parafilm	53.0	55.0	38.8	33.6	18.0	0.727
Dry on parafilm	51.0	55.0	35.9	20.3	5.84	4.81
Dry on paper	59.0	19.9	14.0	6.58	1.73	0.731

Table 4.1: Quantification results of damages produced at different doses on each type of bidosimeters.

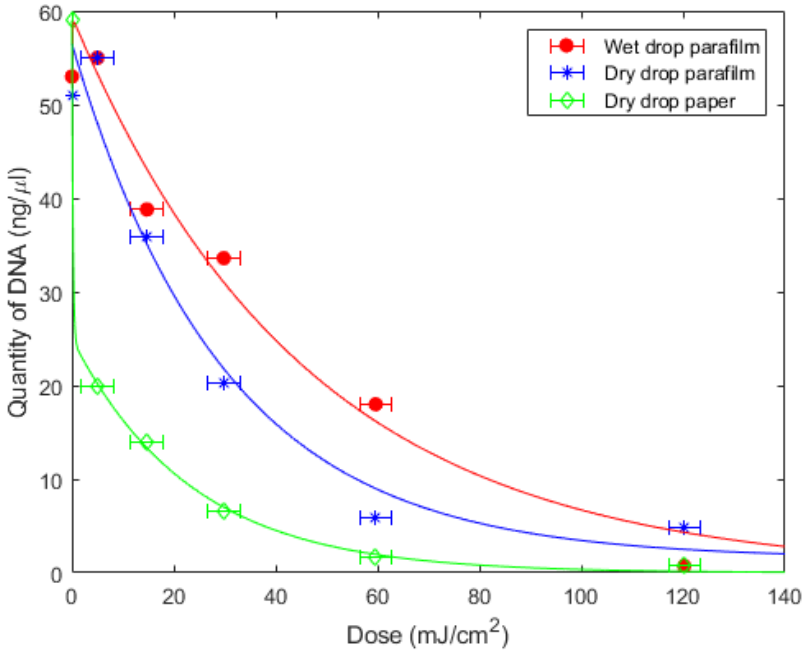

Figure 4.4: Representation of quantification results fitted to a double exponential decay. The amount of amplified DNA over the received UVC dose.

In *Fig. 4.4* the density of DNA is plotted over the received ultraviolet C dose. The more dose the initial sample has received, the more damage it has suffered and the less material the PCR will have to replicate and amplify. Thus, for higher doses the amount of DNA in

quantification is lower.

The error bars of the abscissa axis (in which dose is represented) are obtained by associating a time delay of 3 seconds to turn on and off the lamp, and calculating the corresponding dose variation with the calibration curve. In the case of the ordered axis (in which the quantity of amplified DNA is represented), the error bars are not represented because we cannot estimate it without repeating the procedure much more times. Biological samples vary with conditions such as humidity, temperature or the substrate of the sample, moreover, the sample collection process may lead to variations in the results. By repeating the experiment much more times, the same graph will be obtained with the corresponding error bars in the amount of DNA, improving the quality of the analysis.

At low doses, the effect of radiation is not understood, it seems to be insufficient to damage the sample. For instance, in the parafilm samples with 5 mJ/cm^2 of exposure, the amount of DNA is higher than the non radiated ones, this means that the received dose do not damage the sample, and the difference between 0 and 5 mJ/cm^2 dose should be inside the error because the results do not allow to appreciate a big difference. In the case of paper, the exposition to ultraviolet radiation results in the spreading of tiny drops of sample, which may have a negative impact on the collection of the sample, introducing a larger error in the quantification. This last event also takes place in the wet drop parafilm sample but only at the higher dose, 120 mJ/cm^2.

This *Fig. 4.4* can be also represented in terms of DNA damage as shown in *Fig. 4.5*.

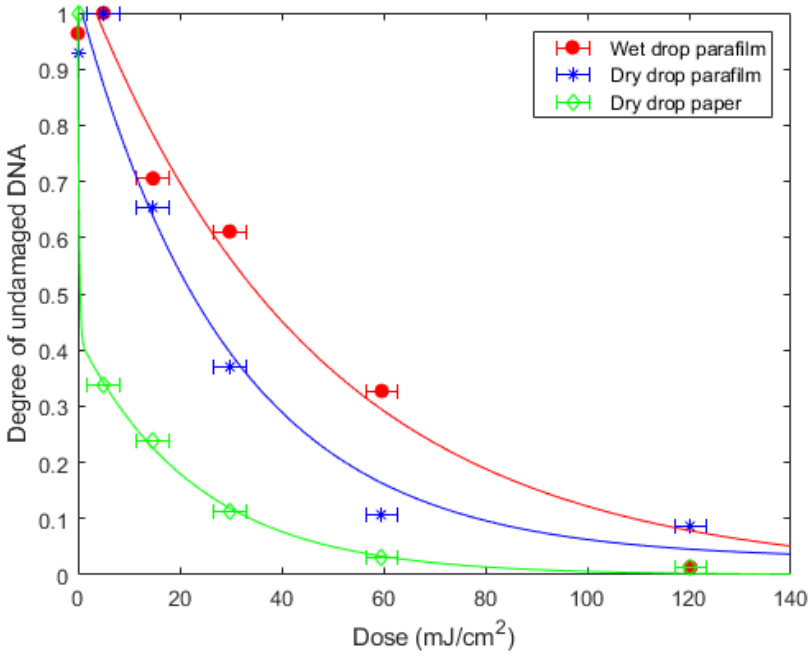

Figure 4.5: Representation of quantification results fitted to a double exponential decay. The undamaged DNA rate over the received UVC dose.

Here, the ordered axis is calculated as the survival fraction, but technically represents the fraction of DNA with no damage, because we are not talking about living organisms but about a component of it, the genetic material. Hence, here the survival fraction can be defined as the opposite of the deactivation rate $\eta = 1 - S$, which is the degree of damage produced in the DNA.

Furthermore, it should be noted that these results do not give the germicidal effect on complex microorganisms, but the effect on their DNA sequence, and the result is not comparable unless both the DNA and the whole microorganism (bacteria, virus,...) are tested and the results analysed, but it serves as a demonstration of the damage caused by UVC radiation on genetic material.

These damage results can also be obtained in a visual way, by using gel electrophoresis technique. To prepare the 2% gel, 2 g agarose powder (from Condalab) is dissolved in 100 ml TBE buffer (reagents from Sigma) by heating it, and then is poured into a cast with a comb. After polymerization, the gel takes the cast form while cooling. Then, the comb is extracted to create wells for loading the samples. Here the TBE buffer is a solution frequently used in electrophoresis, especially in agarose gel to separate nucleic acids. This buffer contains a mixture of Tris base (121.1 g), boric acid (61.8 g), EDTA (7.4 g) and water (1 l).

A reference sample is created for accurate size estimation of DNA fragments, which is composed of 2 μl of DNA ladder, 2 μl of a dye buffer, and 8 μl of distilled water. The samples of study consist of 2 μl of a dye buffer and 10 μl of the previous irradiated and amplified DNA samples. After the gel has been introduced in the electrolytic cell (from Biorad), samples are loaded in the wells and 100V is applied for around 25 minutes to observe the migration of each sample.

Electrophoresis is a molecules separation technique according to their mobility when they are subjected to an electric field. The DNA is a molecule with a negative charge because the sugar-phosphate backbone is negatively charged. Thus, when the electric current is applied, the DNA migrates from the negative pole (cathode) to the positive (anode) through the pores of the gel. The migration velocity will be inversely proportional to the fragment size.

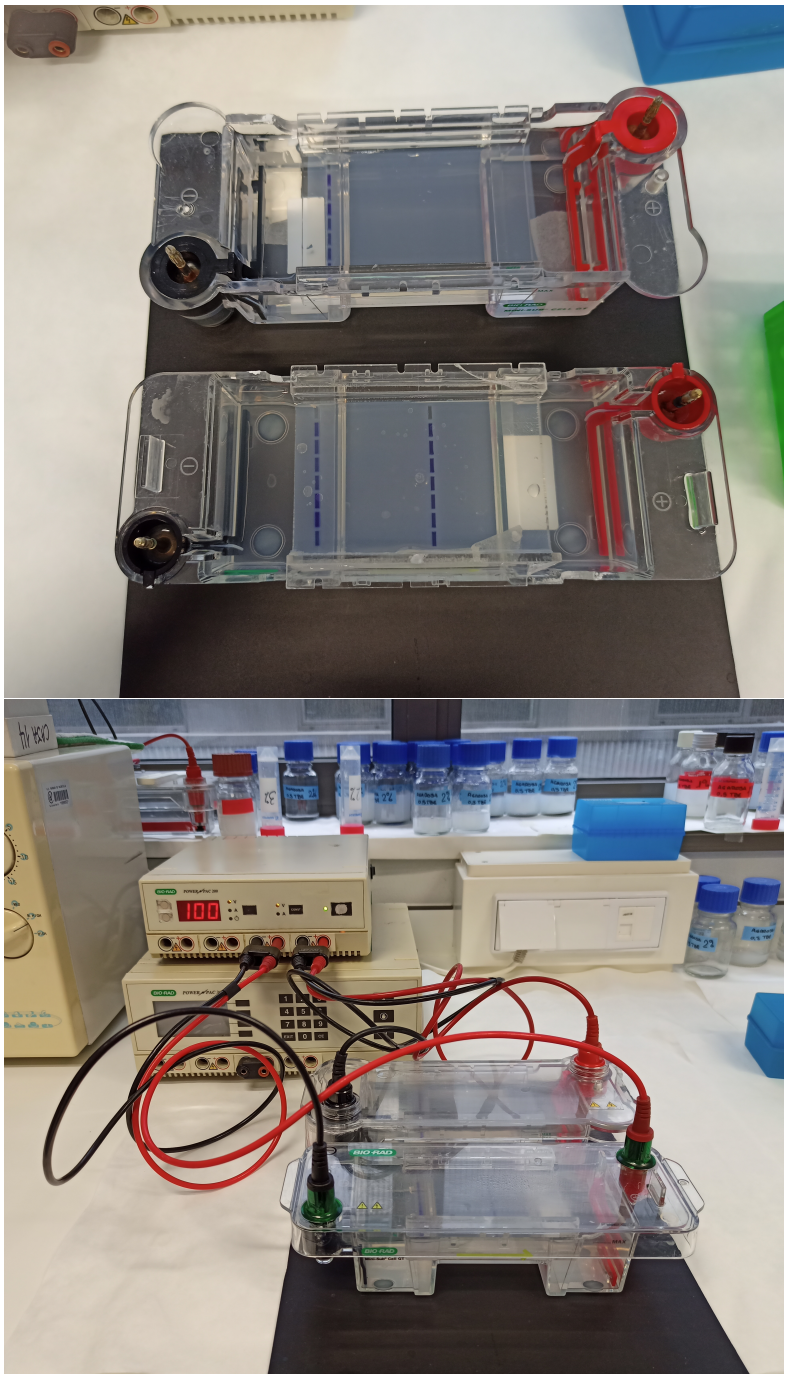

Figure 4.6: Electrophoresis cells with the agarose gel in which wells are loaded with the DNA samples.

When the samples are sufficiently migrated, the results can be seen in a transilluminator, which emits UV light exciting the fluorescence emission of the dye and allowing us to analyse the image through the registered intensity. The results obtained for our samples are shown in *Fig. 4.7*, *Fig. 4.8* and *Fig. 4.9*.

The reference sample is designed to show bands which correspond to 2000, 1200, 800, 400, 200 and 100 bp, in descendent order in the vertical line. Our DNA samples have 1500 bp, which can be shown in the result figures because the bands are between two first of the reference pattern. Moreover, the less intensity, the less quantity of DNA fragments, therefore, the more damage produced in the original DNA sample.

All over those figures, it can be seen that the damage increases with the received UVC dose. Being 60 mJ/cm^2 and 120 mJ/cm^2 doses harmful enough to dramatically slow down DNA replication.

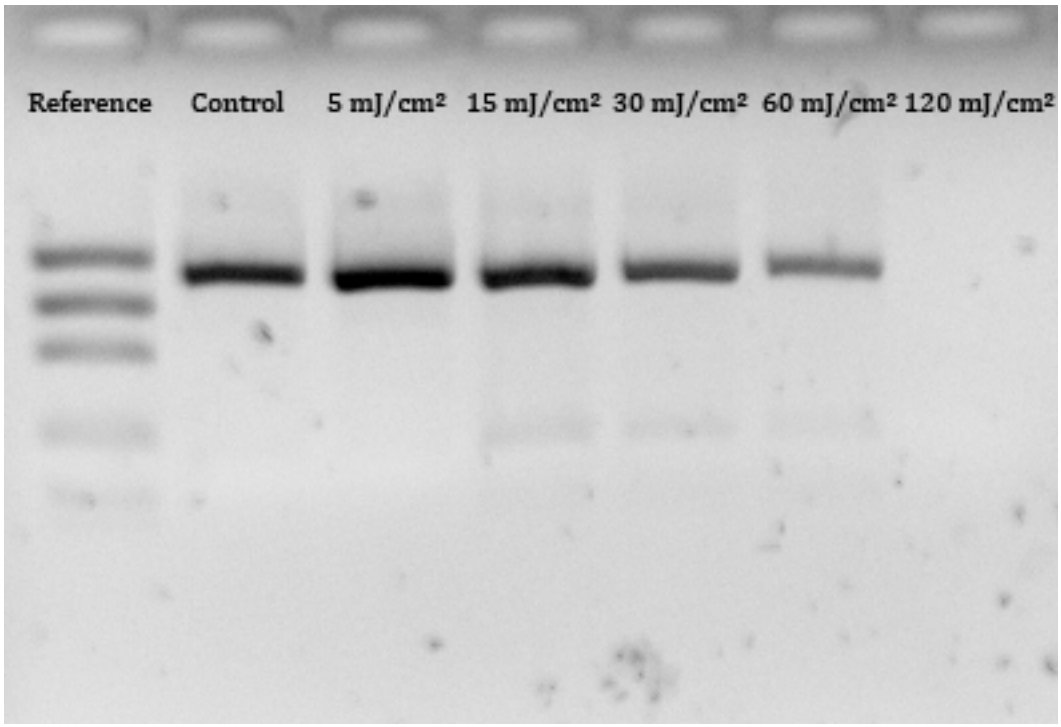

Figure 4.7: Agarose gel electrophoresis image for wet droplets samples on parafilm.

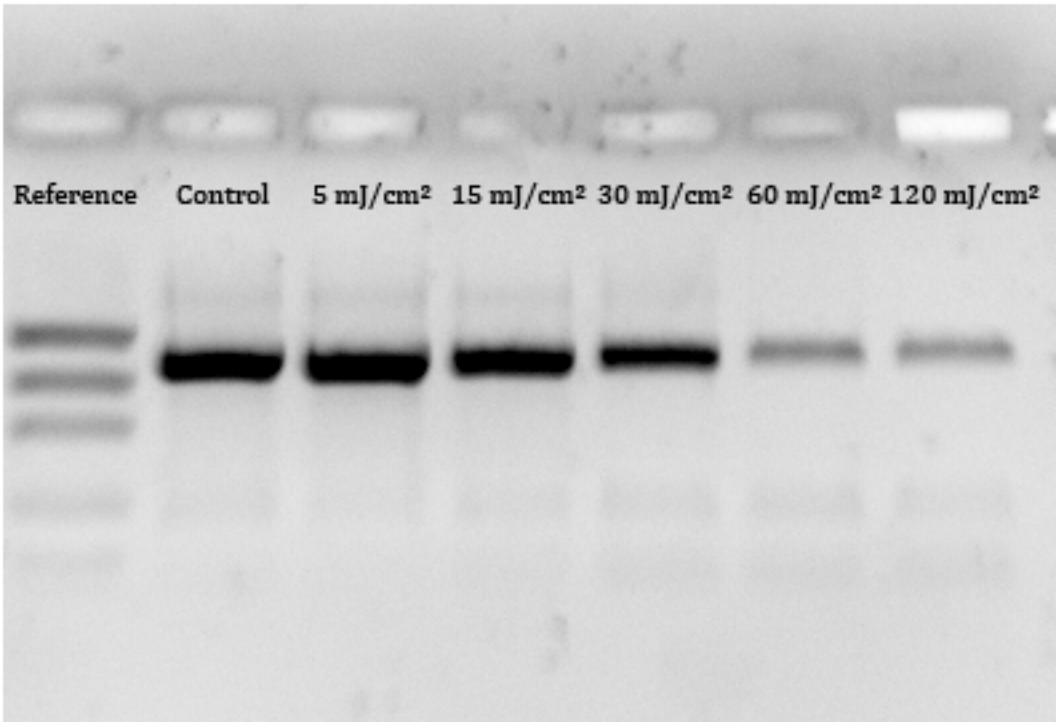

Figure 4.8: Agarose gel electrophoresis image for dry droplets samples on parafilm.

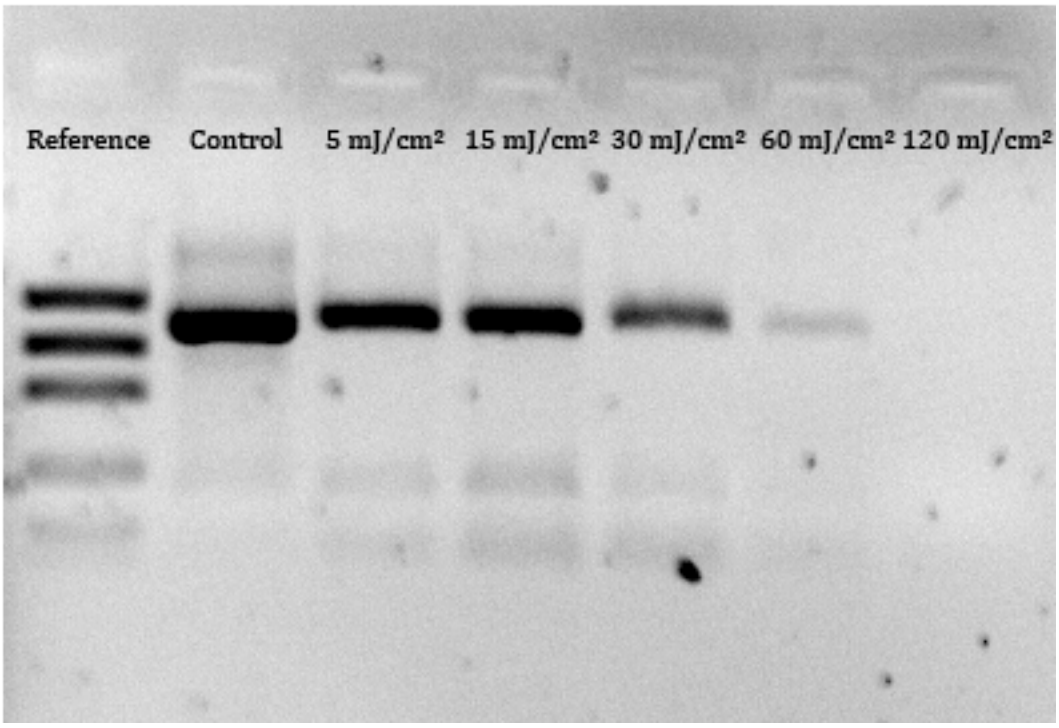

Figure 4.9: Agarose gel electrophoresis image for dry droplets samples on whatman paper.

The results of the irradiated DNA sequence (shown in *Table 4.1*, *Fig. 4.4*, *Fig. 4.5*, *Fig. 4.7*, *Fig. 4.8* and *Fig. 4.9*) make it possible to verify the interaction with ultraviolet C radiation. The DNA is damaged by absorbing UVC radiation, this damage increases with the absorbed dose of UVC and reduces the capability of DNA replication.

By experimentally testing this damage on genetic material, it can be assumed that microorganisms, which carry genetic material in their composition, will also receive damage that can be experimentally quantified in the same way.

In other words, UVC radiation is able to deactivate microorganisms because the genetic material absorbs this radiation. However, many factors will affect the germicidal effect achieved, such as humidity, temperature or the type of microorganism to be deactivated.

Chapter 5

Conclusions and future work

Throughout this thesis, the basis of radiation propagation has been studied and its matter interaction, in order to properly use ultraviolet C radiation as a disinfection tool. Following the procedure to characterize a lamp, simulating and checking the radiation pattern with experimental measurements, the radiometric study can be carried out for any ultraviolet C source, in general with an emission peak in 254 nm, in any room.

The increasing use of ultraviolet C radiation as a disinfection tool in every kind of area, makes it essential to have regulations like those that exist for other ionising radiation, such as X-rays. Although the UVC range is the least energetic of the ionising radiations, exposure to this radiation represents a risk to living organisms, including animals and plants. Therefore, more regulations, warnings and qualified personnel should be required to use ultraviolet radiation devices.

Apart from that ionising radiation sources pass quality controls and cannot be used without adequate radiological protection, one of the best ways to protect oneself is knowledge, in this case, knowing the dose received at each point. As already mentioned, the dose received will depend proportionally on the exposure time and inversely with the distance from the source. In addition, the objects that stand between the subject and the radiation, depending on the material they are made of and their dimensions, may or may not protect us from radiation.

UVC radiation can cause damage to nucleic acids and proteins that can lead to genetic mutation or inactivation of cells. The dose required for inactivation is different for each microorganism, thus, the dose needed to disinfect a surface depends on the selected target and the desired level of disinfection. What is more, ambient conditions, such as humidity and temperature, or the medium in which are embedded can affect the germicidal effect.

Throughout the study of UVC radiation, an effective methodology has been developed to evaluate the germicidal effect of UVC disinfection devices. The process starts with the review of electromagnetic radiation concepts in *Chapter 2* which serves to verify the results of simulations done as indicated in *Section 3.1*. In order to get more realistic results of the radiation pattern, the simulations need to adjust radiation parameters obtained with the lamp characterization (*Section 3.2*) and experimental measurements. To ensure the results of radiation pattern at 254 nm, a radiometer and dosimeters are used. Chemical dosimeters

show results by the colourimetric calibration *Section 3.2.2* and the biodosimeters are useful to analyse the damage caused by the UVC radiation *Section 4.2.2*.

In *Chapter 4* it has been experimentally shown that the genetic material is indeed damaged by absorbing ultraviolet C radiation, hindering or preventing DNA replication. As part of future work, the germicidal effect could be analysed on the entire microorganism and see the damage correlation with the DNA sample. In addition, to complete the biodosimetric analysis, live organisms, such as bacteria, could be used in dosimeters, which after irradiation would be left to incubate, and the number of colonies that grow for the different doses received will represent the survival fraction.

The combination of chemical and biological dosimeters serves as a check of doses in the radiometric study validations of ultraviolet radiation devices, and allows to observe the damage caused to specific pathogens of interest.

In addition to surface disinfection, this technology can be used for water and air disinfection. In fact, the entire study carried out serves as a basis for these other media since the procedure will be the same but taking into account the medium in which the radiation propagates and the fluid dynamics in each case.

Ultraviolet radiation disinfection devices stand out because this technology is fast, free of toxic residues, not specific to one type of microorganism, and its effectiveness does not diminish over time due to the appearance of resistant pathogens. Nevertheless, ultraviolet radiation should never replace sterilization of surgical instruments, and surface disinfection should be applied together with surface cleaning procedures.

Bibliography

[1] David Burnie. *Light*. DK Pub., Inc., 2000.

[2] Philip Hockberger. A history of ultraviolet photobiology for humans, animals and microorganisms. *Photochemistry and photobiology*, 76:561–79, 01 2003.

[3] Wladyslaw Kowalski. *Ultraviolet Germicidal Irradiation Handbook*. Springer, 2009.

[4] Introduction disinfection & sterilization guidelines. `https://www.cdc.gov/infectioncontrol/guidelines/disinfection/introduction.html`, Sep 2016. (last visited 21/06/21).

[5] William A. Rutala and David J. Weber. Disinfection and sterilization in healthcare facilities. In *Practical Healthcare Epidemiology*, pages 58–81. Cambridge University Press, 2018.

[6] Rosemary C. She, Dongyu Chen, Pil Pak, Deniz K. Armani, Andreas Schubert, and Andrea M. Armani. Lightweight UV-c disinfection system. *Biomedical Optics Express*, 11(8):4326, July 2020.

[7] Martin Armbrecht. Detection of contamination in dna and protein samples by photometric measurements. In *Eppendorf*, 2013.

[8] Anthony Griffiths. *Genética*. McGraw-Hill Interamericana, Madrid, 2002.

[9] William Klug. *Concepts of genetics*. Pearson/Prentice Hall, Upper Saddle River, N.J, 2006.

[10] Chang-Hui Shen. Chapter 1 - Nucleic Acids: DNA and RNA. In Chang-Hui Shen, editor, *Diagnostic Molecular Biology*, pages 1–25. Academic Press, 2019.

[11] T Strachan. *Genetics and genomics in medicine*. Garland Science/Taylor & Francis Group, New York, 2015.

[12] R. Nave. Hyperphysics: Electricity and magnetism. `http://hyperphysics.phy-astr.gsu.edu/hbase/Waves/emwavecon.html#c1`. (last visited 04/09/21).

[13] Jonathan A. Jones. Wave conventions: the good, the bad and the ugly. `https://nmr.physics.ox.ac.uk/teaching/wavecon.pdf`. (last visited 17/09/21).

[14] Eugene Hecht. *Optics*. Addison-Wesley, Reading, Mass, 2002.

[15] Justiniano Casas Peláez. *Optica*. Librería Pons, 1994.

[16] James R. Bolton. IUVA News archive. *UV Solutions*, 6(3), 2004.

[17] J.L. Klatte, N. van der Beek, and P.M.J.H. Kemperman. 100 years of wood's lamp revised. *Journal of the European Academy of Dermatology and Venereology*, 29(5):842–847, November 2014.

[18] David H. Sliney, David W. Gilbert, and Terry Lyon. Ultraviolet safety assessments of insect light traps. *Journal of Occupational and Environmental Hygiene*, 13(6):413–424, April 2016.

[19] Multi-probe uv light tester application and usage. `https://www.linshangtech.com/tech/multi-probe-uv-light-tester-application-and-usage-tech1287.html`. (last visited 04/08/21).

[20] Javier García Fernández and Oriol Boix. Lámparas y luminarias. `https://recursos.citcea.upc.edu/llum/lamparas/lamp0.html`. (last visited 22/06/21).

[21] Shamim I. Ahmad, Luisa Christensen, and Elma Baron. *History of UV Lamps, Types, and Their Applications*, pages 3–11. Springer International Publishing, Cham, 2017.

[22] Sulaiman Khan, David Newport, and Stéphane Le Calvé. Gas detection using portable deep-UV absorption spectrophotometry: A review. *Sensors*, 19(23):5210, November 2019.

[23] Shelly L. Miller, Jacqueline Linnes, and Julia Luongo. Ultraviolet germicidal irradiation: Future directions for air disinfection and building applications. *Photochemistry and Photobiology*, 89(4):777–781, 2013.

[24] Wenshan Cai. *Optical metamaterials : fundamentals and applications*. Springer, New York London, 2009.

[25] I.F. Almong, M.S. Bradley, and V. Bulović. The Lorentz Oscillator and its Applications. MIT OpenCourseWare. `https://ocw.mit.edu/courses/electrical-engineering-and-computer-science/6-007-electromagnetic-energy-from-motors-to-lasers-spring-2011/readings/MIT6_007S11_lorentz.pdf`. (last visited 17/09/21).

[26] Ack. Ozone formation and destruction. `https://cimss.ssec.wisc.edu/wxwise/ozone/OZONE2.html`. (last visited 13/07/21).

[27] Martin Purschke, Mazzin Elsamaloty, Jeffrey Wilde, Nichole Starr, Rox Anderson, William Farinelli, Fernanda Sakamoto, Maryann Tung, Joshua Tam, Lambertus Hesselink, and Thomas Baer. Construction and validation of uv-c decontamination cabinets for filtering facepiece respirators. *Applied Optics*, 07 2020.

[28] Holger Claus. Ozone generation by ultraviolet lamps†. *Photochemistry and Photobiology*, 97(3):471–476, 2021.

[29] William A. Rutala. Disinfection & sterilization. `https://disinfectionandsterilization.org/`. (last visited 27/07/21).

[30] Chih-Shan Li and Yu-Chun Wang. Surface germicidal effects of ozone for microorganisms. *AIHA Journal*, 64(4):533–537, July 2003.

[31] LLC LTI Optics. We are optical design. https://www.ltioptics.com/en/. (last visited 14/07/21).

[32] Yousra M. Ahmed, Mark Jongewaard, Mengkai Li, and Ernest R. Blatchley. Ray tracing for fluence rate simulations in ultraviolet photoreactors. *Environmental Science & Technology*, 52(8):4738–4745, March 2018.

[33] Busse Margaret M. Characterization of a continuous-flow reactor for solar uv water disinfection. https://docs.lib.purdue.edu/open_access_theses/755, 2016. (last visited 13/07/21).

[34] Josephine Lau, William Bahnfleth, Richard Mistrick, and Diana Kompare. Ultraviolet irradiance measurement and modeling for evaluating the effectiveness of in-duct ultraviolet germicidal irradiation devices. *HVAC&R Research*, 18(4):626–642, 2012.

[35] Wladyslaw Kowalski and William Bahnfleth. Uvgi design basics for air and surface disinfection. *HPAC Heating, Piping, Air Conditioning*, 72:10 pp, 01 2000.

[36] UVC light meter datalogger, type k/j thermometer, up to 254 nm. https://www.mrclab.com/uvc-light-meterdatalogger-type-kj-thermometer. (last visited 16/07/21).

[37] TUV PL-S 9W/2P 1CT/6X10BOX. https://www.lighting.philips.com/main/prof/conventional-lamps-and-tubes/special-lamps/purificationwater-and-air/residential-water-and-air/tuv-pl-s/927901704007_EU/product. (last visited 07/08/21).

[38] Marie Lindblad, Eva Tano, Claes Lindahl, and Fredrik Huss. Ultraviolet-C decontamination of a hospital room: Amount of UV light needed. *Burns*, 46(4):842–849, 2020.

[39] When it comes to uv-c disinfection, seeing is believing. =https://uvcdosimeters.com/. (last visited 12/08/21).

[40] Konica Minolta Sensing. Medidor de colorimetría CR-400. https://sensing.konicaminolta.us/mx/products/cr-400-chroma-meter-colorimeter. (last visited 12/08/21).

[41] Konica Minolta Color, Light, and Display Measuring Instruments. What is CIE 1976 Lab Color Space? https://sensing.konicaminolta.asia/what-is-cie-1976-lab-color-space/. (last visited 12/08/21).

[42] Stefan Källberg. UVC exposure (254 nm) of uv sensitive material at different irradiation levels. https://uvcdosimeters.com/wp-content/uploads/2020/05/RISE_report_Intellego_UVCdoimeter_100.pdf. (last visited 10/08/21).

[43] Bao Ly, Ethan Dyer, Jessica Feig, Anna Chien, and Sandra Bino. Research techniques made simple: Cutaneous colorimetry: A reliable technique for objective skin color measurement. *The Journal of investigative dermatology*, 140:3–12.e1, 01 2020.

[44] Christine Cotton and James Bolton. *The ultraviolet disinfection handbook*. American Water Works Association, Denver, CO, 2008.

[45] UV-C for hvac air and surface disinfection. https://www.amca.org/educate/articles-and-technical-papers/amca-inmotion-articles/uv-c-for-hvac-air-and-surface-disinfection-2.html. (last visited 04/08/21).

[46] *ASHRAE handbook: heating, ventilating, and air-conditioning applications*. ASHRAE, Atlanta, Ga, 2015. Chapter 60.

[47] Ursinio Puga Gil. Ultraviolet Disinfection Pilot Study at the Fargo Wastewater Treatment Plant. *North Dakota State University*, April 2017.

[48] Acharya Tankeshwar, Rabia Ali says:, Arif says:, Sehrish aslam says:, Bushra Ali says:, Haseeb Ahmad Ayazi says:, Faiz ul hassan says:, Akshay says:, Raj singh says:, Sandy says:, and et al. Polymerase chain reaction (pcr): Steps, types, applications • microbe online, Jul 2021.

[49] Polymerase chain reaction. https://en.wikipedia.org/wiki/Polymerase_chain_reaction. (last visited 25/08/21).

[50] R.A. Rodríguez, S. Bounty, and K.G. Linden. Long-range quantitative pcr for determining inactivation of adenovirus 2 by ultraviolet light. *Journal of Applied Microbiology*, 114(6):1854–1865, 2013.

Appendix A

Luminaire geometry

The diagram which represents the dimensions of luminaire used all over this work is shown below.

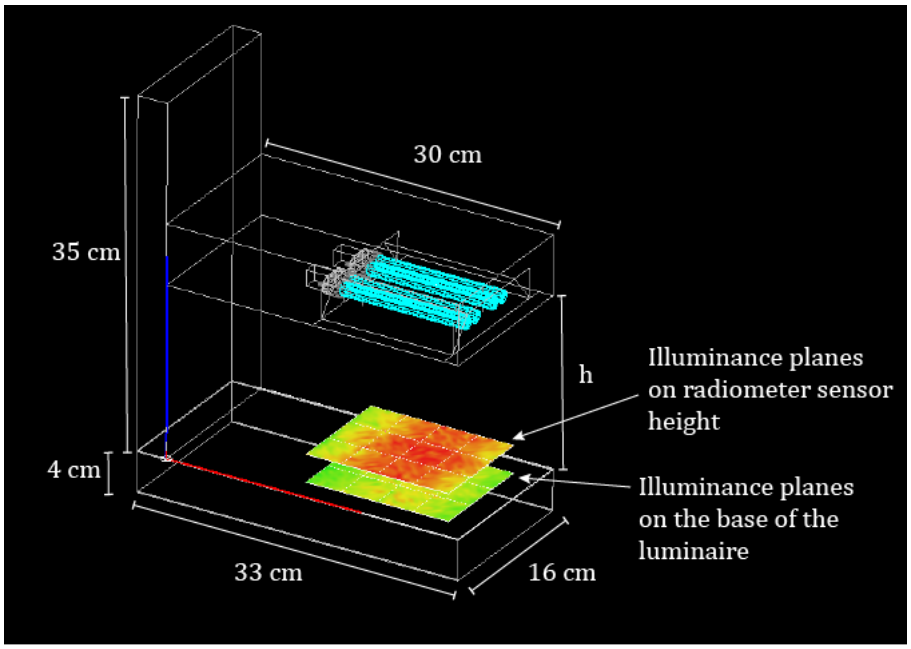

Position	$h_{position}$ (cm)
1	1.1
2	3.1
3	5.2
4	7.1
5	9
6	11.1
7	13
8	15.1
9	17.1
10	19.1
11	21
12	23.1
13	25
14	27

Figure A.1: Diagram of luminaire used for calibration showing the lamps on cyan and the illuminance planes in the base and at the height in which the radiometer measures. Along with it, a table contains the different heights at which one can adjust the movable part where the lamps are located.

The illuminance plane on radiometer sensor height is included in the simulation because the radiometer used has size, a diameter of 3.67 cm and a height of 2.75 cm.

In *Fig. A.2* a top view of the luminaire is shown to specify the position to place the radiometer and measure a map of irradiances.

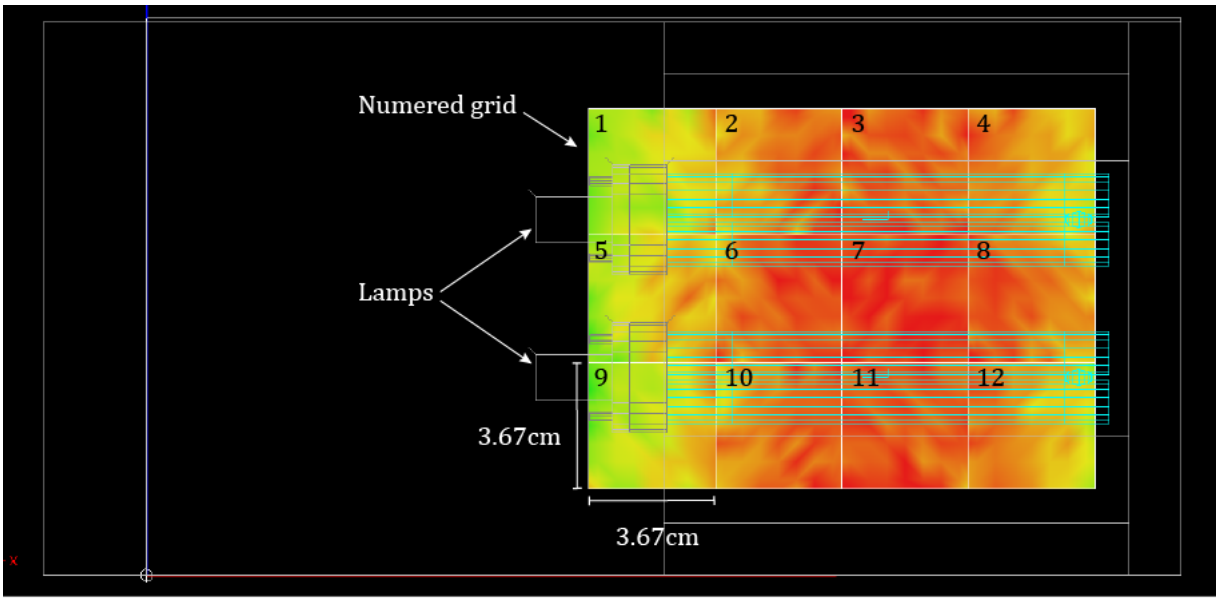

Figure A.2: Measurement grid in the base of the lamp used to place the radiometer and create a map of irradiance.

Appendix B

Irradiation protocol

The irradiation of the samples has always been done following the same procedure in order to expose the samples to as precise a dose as possible. The procedure starts with the luminaire being switched on for 6 minutes, then kept off for two minutes, and then the samples are irradiated.

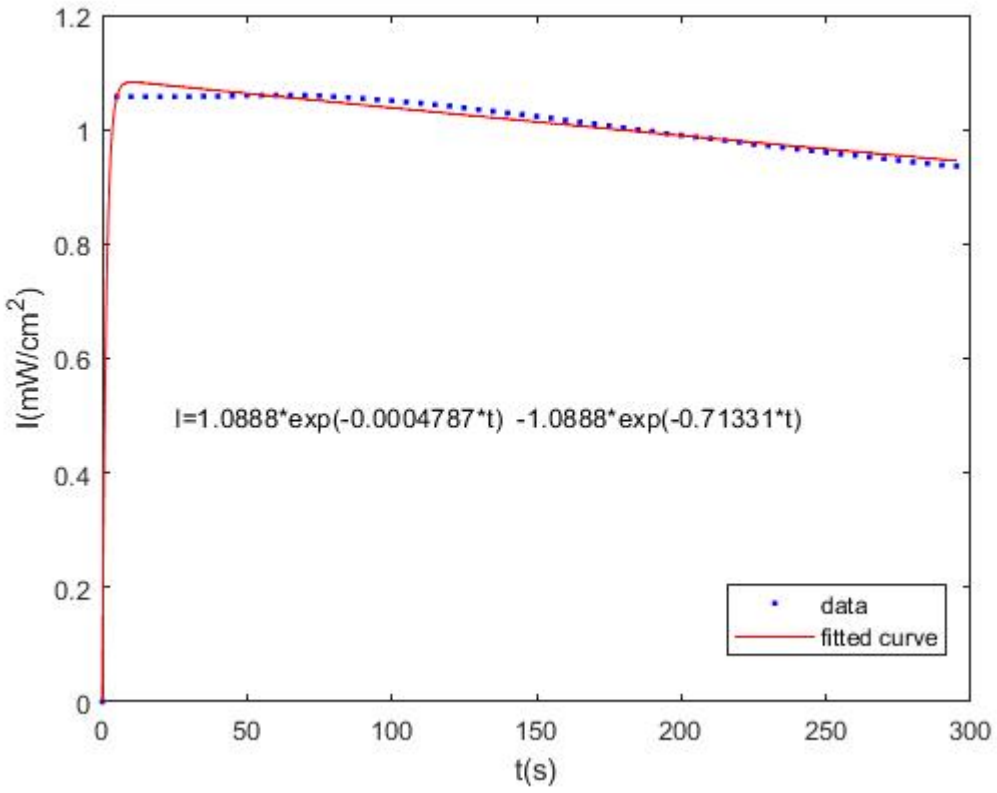

Figure B.1: Irradiation in position 7 of the base of the luminaire for 5 minutes. the integration of this curve, and its fit, allows us to obtain the dose received during a fixed exposure time.

To calculate the dose, the radiometer is placed in position 7 with the lamps at height 14 (see Appendix *A*), where the sample will be placed, obtaining the irradiation every 5 seconds during 5 minutes, this curve is represented in *Fig. B.1*.

Position 7, Height 14	
time (s)	Dose (mJ/cm^2)
0	0
6	5.0116
15	14.7324
29	29.804
57	59.6485
115	120.221

Table B.1: Received dose in a specific point during different times based on Fig. B.1.

Appendix C

Matlab codes

Function code that gives the received dose for the colour measured in the chemical dosimeter.

```
function [dosis]=DosisColorimetro(Ls,as,bs)
    color=[88.81 -7.82 50.64; %0mJ/cm^2 amarillo
        88.83 -7.90 49.88; %0mJ/cm^2
        88.76 -7.87 49.93; %0mJ/cm^2
        84.78 -0.92 42.47; %5mJ/cm^2
        84.78 -0.92 42.40; %5mJ/cm^2
        84.78 -0.97 42.44; %5mJ/cm^2
        84.91 -1.13 42.54; %5mJ/cm^2
        88.26 -7.52 52.80; %0mJ/cm^2
        81.30 5.29 34.55; %10.4mJ/cm^2
        81.19 5.46 34.44; %10.4mJ/cm^2
        81.11 5.55 34.59; %10.4mJ/cm^2
        81.30 5.39 34.39; %10.4mJ/cm^2
        81.16 5.51 34.59; %10.4mJ/cm^2
        88.32 -7.57 52.76; %0mJ/cm^2
        88.31 -7.56 52.76; %0mJ/cm^2
        78.80 8.67 33.72; %14.7mJ/cm^2
        78.75 8.75 33.93; %14.7mJ/cm^2
        78.86 8.68 33.21; %14.7mJ/cm^2
        78.86 8.67 33.45; %14.7mJ/cm^2
        78.86 8.68 33.31; %14.7mJ/cm^2
        88.37 -7.59 52.57; %0mJ/cm^2
        77.63 10.95 30.23; %20.1mJ/cm^2
        77.58 11.10 29.62; %20.1mJ/cm^2
        77.38 11.35 30.08; %20.1mJ/cm^2
        77.37 11.40 29.92; %20.1mJ/cm^2
        77.44 11.31 29.41; %20.1mJ/cm^2
        87.91 -7.78 50.72; %0mJ/cm^2 CERO DE REFERENCIA
        87.88 -7.73 50.86; %0mJ/cm^2
        75.71 13.76 24.59; %25.5mJ/cm^2
        75.63 13.84 24.73; %25.5mJ/cm^2
        75.55 14.07 24.68; %25.5mJ/cm^2
        75.50 14.09 24.36; %25.5mJ/cm^2
        75.50 14.12 24.37; %25.5mJ/cm^2
```

```
        74.32 14.69 25.52; %29.8mJ/cm^2
        74.47 14.69 24.92; %29.8mJ/cm^2
        74.52 14.64 24.76; %29.8mJ/cm^2
        74.32 14.84 25.24; %29.8mJ/cm^2
        74.32 14.89 24.93; %29.8mJ/cm^2
        88.79 -7.89 50.96; %0mJ/cm^2
        73.25 18.58 21.50; %35.1mJ/cm^2
        73.04 18.77 21.07; %35.1mJ/cm^2
        73.18 18.78 20.97; %35.1mJ/cm^2
        73.15 18.86 21.13; %35.1mJ/cm^2
        72.87 18.72 20.56; %35.1mJ/cm^2
        73.83 18.91 17.88; %40.5mJ/cm^2
        73.75 18.97 18.07; %40.5mJ/cm^2
        73.49 19.38 17.81; %40.5mJ/cm^2
        73.58 19.31 17.49; %40.5mJ/cm^2
        73.58 19.23 17.72; %40.5mJ/cm^2
        71.00 21.25 17.31; %50.1mJ/cm^2
        70.95 21.28 17.26; %50.1mJ/cm^2
        71.09 21.37 16.59; %50.1mJ/cm^2
        70.79 21.66 16.85; %50.1mJ/cm^2
        70.86 21.58 16.77; %50.1mJ/cm^2
        70.21 23.79 13.24; %60.7mJ/cm^2
        70.21 23.95 13.06; %60.7mJ/cm^2
        70.06 24.21 13.17; %60.7mJ/cm^2
        69.92 24.28 13.04; %60.7mJ/cm^2
        70.08 24.18 12.82; %60.7mJ/cm^2
        68.57 25.52 13.78; %70.2mJ/cm^2
        68.65 25.36 13.60; %70.2mJ/cm^2
        68.25 25.91 13.22; %70.2mJ/cm^2
        68.23 26.07 12.72; %70.2mJ/cm^2
        68.22 26.04 13.23; %70.2mJ/cm^2
        68.18 27.03 9.04; %80.7mJ/cm^2
        67.89 27.30 8.79; %80.7mJ/cm^2
        68.05 27.26 8.36; %80.7mJ/cm^2
        67.92 27.21 8.91; %80.7mJ/cm^2
        67.94 27.39 8.45; %80.7mJ/cm^2
        67.60 29.36 7.84; %90.2mJ/cm^2
        67.60 29.56 7.53; %90.2mJ/cm^2
        67.52 29.63 7.39; %90.2mJ/cm^2
        67.37 29.83 7.57; %90.2mJ/cm^2
        67.39 29.39 7.32; %90.2mJ/cm^2
        66.75 30.48 5.85; %100.6mJ/cm^2
        66.68 30.59 5.93; %100.6mJ/cm^2
        66.78 30.64 5.40; %100.6mJ/cm^2
        66.66 30.73 5.36; %100.6mJ/cm^2
        66.61 30.82 5.37; %100.6mJ/cm^2
        67.36 32.10 -3.64; %149.9mJ/cm^2
        67.16 32.37 -3.49; %149.9mJ/cm^2
        67.09 32.40 -3.31; %149.9mJ/cm^2
        67.22 32.27 -3.54; %149.9mJ/cm^2
        67.08 32.35 -3.42; %149.9mJ/cm^2
        63.77 36.05 -5.79; %200.1mJ/cm^2
        63.92 35.91 -5.75; %200.1mJ/cm^2
```

```
        63.87 35.94 -5.73; %200.1mJ/cm^2
        63.85 35.99 -5.83; %200.1mJ/cm^2
        63.78 36.01 -5.65; %200.1mJ/cm^2
        62.55 37.79 -6.85; %250.1mJ/cm^2
        62.38 37.94 -6.75; %250.1mJ/cm^2
        62.65 37.64 -6.80; %250.1mJ/cm^2
        62.79 37.54 -6.95; %250.1mJ/cm^2
        62.56 37.70 -6.79; %250.1mJ/cm^2
        66.10 30.98 2.60;%120.3mJ/cm^2
        65.95 31.10 2.70;%120.3mJ/cm^2
        66.01 31.08 2.61;%120.3mJ/cm^2
        66.19 30.84 2.30;%120.3mJ/cm^2
        66.37 30.75 2.21;%120.3mJ/cm^2
        65.50 32.46 1.99; %135.6mJ/cm^2
        65.06 32.82 2.47; %135.6mJ/cm^2
        65.24 32.67 2.16; %135.6mJ/cm^2
        65.38 32.60 2.00; %135.6mJ/cm^2
        65.18 32.79 2.32; %135.6mJ/cm^2
        65.28 34.98 -3.58; %175.1mJ/cm^2
        65.04 35.25 -3.48; %175.1mJ/cm^2
        65.16 35.06 -3.59; %175.1mJ/cm^2
        65.30 34.97 -3.69; %175.1mJ/cm^2
        65.14 35.15 -3.58; %175.1mJ/cm^2
        65.82 32.73 0.14; %142.8mJ/cm^2
        65.62 32.98 0.31; %142.8mJ/cm^2
        65.66 32.93 0.27; %142.8mJ/cm^2
        65.58 33.02 0.24; %142.8mJ/cm^2
        65.60 32.99 0.29]; %142.8mJ/cm^2

    for i=1:114
        Lab_s=lab2xyz([color(i,:)]);
        X0=Lab_s(1);
        Y0=Lab_s(2);
        Z0=Lab_s(3);
        x(i)=X0/(X0+Y0+Z0);
        y(i)=Y0/(X0+Y0+Z0);
    end

    D=[0 0 0 5.1 5.1 5.1 5.1 0 10.4 10.4 10.4 10.4 10.4 0 0 14.7 14.7 14.7 14.7 14.7
        ↪  0 20.1 20.1 20.1 20.1 20.1 0 0 25.5 25.5 25.5 25.5 25.5 29.8 29.8 29.8
        ↪ 29.8 29.8 0 35.1 35.1 35.1 35.1 35.1 40.5 40.5 40.5 40.5 40.5 50.1 50.1
        ↪ 50.1 50.1 50.1 60.7 60.7 60.7 60.7 60.7 70.2 70.2 70.2 70.2 70.2 80.7 80.7
        ↪  80.7 80.7 80.7 90.2 90.2 90.2 90.2 90.2 100.6 100.6 100.6 100.6 100.6
        ↪ 149.9 149.9 149.9 149.9 149.9 200.1 200.1 200.1 200.1 200.1 250.1 250.1
        ↪ 250.1 250.1 250.1 120.3 120.3 120.3 120.3 120.3 135.6 135.6 135.6 135.6
        ↪ 135.6 175.1 175.1 175.1 175.1 175.1 142.8 142.8 142.8 142.8 142.8];
    % Ajuste DeltaE* respecto amarillo L*=87.91 a*=-7.78 b*=50.72
    for i=1:114
        DL_star=color(i,1)-color(27,1);
        Da_star=color(i,2)-color(27,2);
        Db_star=color(i,3)-color(27,3);
        DE_star(i)=sqrt((DL_star)^2+(Da_star)^2+(Db_star)^2);
    end
```

```
    f1=fit(DE_star',D','exp2');
    v1= coeffvalues(f1);

    DLs=Ls-color(27,1);
    Das=as-color(27,2);
    Dbs=bs-color(27,3);
    DEs=sqrt((DLs)^2+(Das)^2+(Dbs)^2);
    dosis=v1(1)*exp(v1(2)*DEs) + v1(3)*exp(v1(4)*DEs);
end
```

Appendix D

Gene sequencing

ODZ1 - ENSEMBL transcript ID: ENST00000422452.2 (translated strand)

```
1 cacgaggtgaggagatcgagaccatcctggctaacttggtgaaatcccgtctctactaaaaatacaaaa
    ↪ aaaattagccgggcatggtggcgggtgcctgtagtcctagctactcgggaggctgaggcagaagaatgg
    ↪ cgtgaacccgggagacggagcttgcagtgagccgagatcgcaccactgaactccagcctgggcgactga
    ↪ gcaagactccgtctctaaatcaatcaatcaatcaatcaatcaaattgatcaataaaaatcagcctacat
    ↪ catactttgaaaagctaaaagccttttttgaatgatttctgtgttctatgtgcttggcataaatgcaat
    ↪ aagaattccaaaatatgagatagtgtacatgatagaggagccaccatttggatgtctatagatttcttt
    ↪ gaaaatacatatggtgaagagctgaagaaaaataaaagagtcagtttcactgcaaaataaaatcataaa
    ↪ gttaattggtttctaactacatttttaaacattgtatgaaaagaccaagttgcaaagttgcaacagtgg
    ↪ actgaaatggtgatgacaaaataatgtaaagaatgaaaataagaacatttttacagggcttttaaattt
    ↪ acagaggactttgacatctcagatgacacttgatcgtctcgaaactctccgtgctaagtagagcagtta
    ↪ atgcctctactggccctaagaccttcagtggctcctagctcagcattctatggggaaaggggttcttt
    ↪ cggtgatttatcatgaagtttaaaattgctatttccaaaactgatttagatcctgctgttgctgtacca
    ↪ gtatactcaccagaagtgtttacatcctctcagtactatgaagaacaaaaatttaccaccacctaactc
    ↪ attaagaatgctctgcaggcctgaggctcaaaagccacaatatgagcacaaagagttcagtccccctca
    ↪ aggatactttattccatgagctctctcactcagaatccttcccttactcagagcccctgtcttaaatgt
    ↪ aatattaaaccagaagcaagaatgtgttctttctgaatgtagttctcttaccagttttcatttcaaatg
    ↪ tggaatgtgcagggttaatctttgtactcctcaccactttcaaatctgataacgtttttaatctaacc
    ↪ actgattttaacattaaaaacacgcacacaccatagaacaacgttgtcctctatttgaattccaataca
    ↪ aatatttttgaaggctgtctctcttttaccttgagtattttctgatgctgcaacctccagcttaatcct
    ↪ taatgcttgacaatgtatgcatgtaacacagagtgttattattgcctccggctagcttcatgtcatcta
    ↪ gtttgtcttttacttctctcctttgatggtattatcaggaccaattgtgaatctgccagatgcatttcc
    ↪ tcacaaaaagataaatctaagaaggcttgtgtttttccctttctcttccag
```